

# Quinoxaline-Based D–A Copolymers for the Applications as Polymer Donor and Hole Transport Material in Polymer/Perovskite Solar Cells

Chenkai Sun,\* Can Zhu, Lei Meng, and Yongfang Li\*

Dedicated to Prof. Daoben Zhu for celebrating his 80<sup>th</sup> birthday

Polymer solar cells (PSCs) have achieved great progress recently, benefiting from the rapid development of narrow bandgap small molecule acceptors and wide bandgap conjugated polymer donors. Among the polymer donors, the D–A copolymers with quinoxaline (Qx) as A-unit have received increasing attention since the report of the low-cost and high-performance D–A copolymer donor based on thiophene D-unit and difluoro-quinoxaline A-unit in 2018. In addition, the weak electron-deficient characteristic and the multiple substitution positions of the Qx unit make it an ideal A-unit in constructing the wide bandgap polymer donors with different functional substitutions. In this review article, recent developments of the Qx-based D–A copolymer donors, including synthetic method of the Qx unit, backbone modulation, side chain optimization, and functional substitution of the Qx-based D–A copolymers, are summarized and discussed. Furthermore, the application of the Qx-based D–A copolymers as hole transport material in perovskite solar cells (pero-SCs) is also introduced. The focus mainly on the molecular design strategies and structure–properties relationship of the Qx-based D–A copolymers, aiming to provide a guideline for developing high-performance Qx-based D–A copolymers for the applications as donor in PSCs and as hole transport material in pero-SCs.

## 1. Introduction

The accelerating consumption of fossil energy source due to the increasing energy demand has caused the global environmental pollution and greenhouse gas problem, which has forced us to exploit and use clean sustainable energy in recent years. Among the sustainable energy, solar energy has received widespread attentions from all over the world because of its inherent advantages of clean and inexhaustible. Solar cells, which directly converts light energy into electricity, is one of the most important technology of solar energy utilization, and has developed rapidly in the past twenty years. Especially the silicon-based solar cells have realized large scale application, and the polymer solar cells (PSCs) and perovskite solar cells (pero-SCs) have developed quickly in recent years.

PSCs, one of the third-generation solar cell technology, are composed of a blend photoactive layer of a *p*-type conjugated polymer as electron donor and an *n*-type organic semiconductor (*n*-OS) as electron acceptor sandwiched between a bottom transparent electrode and a top metal electrode. The PSCs have attracted intensive attentions and achieved rapid development because of its intrinsic advantages of low-cost fabrication by solution processing, simple device structure, light weight, and capability to be fabricated into flexible and semi-transparent devices.<sup>[1–5]</sup>

In general, a high-efficiency PSC is the synergistic result of high open-circuit voltage ( $V_{oc}$ ), large short-circuit current density ( $J_{sc}$ ), and high fill factor (FF), and the power conversion efficiency (PCE) of the PSCs is defined as  $PCE = V_{oc} \times J_{sc} \times FF / P_{light}$ , where  $P_{light}$  is the light intensity of the irradiated light during the measurement.<sup>[6]</sup> The  $V_{oc}$  values of the PSCs are proportional to the energy level difference between the lowest unoccupied molecular orbital (LUMO) of the acceptor and the highest occupied molecular orbital (HOMO) of the donor, the  $J_{sc}$  values depend on the absorption spectra and the excitons dissociation and charge transportation efficiencies of the donor and acceptor photovoltaic materials, and FF values are related to the charge transportation and charge recombination behavior of the photoactive layer of the PSCs. In order to realize high PCE, therefore, it is crucial for the donor (D)/acceptor (A) photovoltaic

C. Sun, C. Zhu, L. Meng, Y. Li  
Beijing National Laboratory for Molecular Sciences  
CAS Key Laboratory of Organic Solids  
Institute of Chemistry  
Chinese Academy of Sciences  
Beijing 100190, China  
E-mail: schenkai@zsu.edu.cn; liyf@iccas.ac.cn

C. Sun  
College of Chemistry, and Green Catalysis Center  
Zhengzhou University  
Zhengzhou 450001, China

C. Sun, C. Zhu, Y. Li  
School of Chemical Science  
University of Chinese Academy of Sciences  
Beijing 100049, China

Y. Li  
Laboratory of Advanced Optoelectronic Materials  
Suzhou Key Laboratory of Novel Semiconductor-Optoelectronics  
Materials and Devices  
College of Chemistry  
Chemical Engineering and Materials Science  
Soochow University  
Suzhou 215123, China

 The ORCID identification number(s) for the author(s) of this article can be found under <https://doi.org/10.1002/adma.202104161>.

DOI: 10.1002/adma.202104161

materials pair of the PSCs to possess a) the suitable electronic energy levels alignment to achieve high  $V_{oc}$  and to afford sufficient driving force for efficient charge separation with low voltage loss ( $V_{loss}$ ) simultaneously; b) the broad and complementary absorption spectra with high extinction coefficients in the visible-near infrared region to harvest more solar photons; and c) the D/A bi-continuous interpenetrating network morphology with appropriate nanoscale phase separation and high charge mobility to facilitate exciton dissociation and charge transport.<sup>[2,7–10]</sup> To meet these requirements, researchers have developed plenty of efficient photovoltaic molecules (including *p*-type conjugated polymer donors<sup>[2,10]</sup> and *n*-OS acceptors<sup>[11–13]</sup>) through subtle molecular structure optimization.

Before 2015, fullerene derivatives (such as PC<sub>61</sub>BM, PC<sub>71</sub>BM,<sup>[11]</sup> and ICBA<sup>[14]</sup>) were the most widely used *n*-OS acceptors due to their excellent electron transport characteristics and strong electron-deficient properties. The PCEs of the PSCs with the fullerene derivative as electron acceptor exceed 10% in 2015 when combined with a narrow bandgap polymer donor.<sup>[15]</sup> However, the fullerene derivative acceptors suffer from inherent shortcomings of weak visible light absorption and difficulty in tuning the light absorption and electronic energy levels, which limits further improvement of the PCEs. The appearance of the narrow bandgap nonfullerene *n*-OS small molecule acceptors overcome the limitation of the fullerene derivative acceptors and have driven rapid development of the PSCs in recent years.<sup>[4,5,12,13]</sup> Especially, the A–DA'D–A structured narrow bandgap acceptor Y6<sup>[13]</sup> and its derivatives have promoted the PCEs of the PSCs to over 17–18% recently.

In addition to the rapid development of the narrow bandgap acceptors, the continuous innovations of the wide bandgap conjugated polymer donors also give great contribution for the photovoltaic performance improvements of the PSCs.<sup>[10,16,17]</sup> Among the molecular design strategies of the polymer donors, the D–A copolymerization of electron donating (D) unit and electron accepting (A) unit has proven to be the most important and effective approach for constructing high performance polymer donors since it was proposed in 1992,<sup>[18]</sup> and almost all the highly efficient polymer donors for the PSCs are designed based on the D–A strategy nowadays. The optical and electronic properties of the D–A copolymers can be easily tuned by controlling the intramolecular charge transfer (ICT) from the D unit to the A unit.<sup>[19]</sup> With this approach, numerous highly efficient D–A copolymer donors are developed by incorporating various functionalized electron-rich D-units (such as thiophene, bithiophene, fluorene, benzodithiophene (BDT), etc.) with functionalized electron-deficient A-units (such as benzothiadiazole (BT), benzotriazole (BTz), benzo-[1,2-*c*:4,5-*c'*]dithiophene-4,8-dione (BDD), quinoxaline (Qx), etc.).<sup>[6,10]</sup>

Qx and its derivatives are a class of widely used A-blocks to construct the D–A copolymers because of their remarkable merits,<sup>[20]</sup> including the weak electron-deficient characteristic, strong quinoid form, and the multiple substitution positions (2, 3, 6, 7 positions) of the Qx unit (Scheme 1a). The weak electron-deficient characteristic of the A-unit is favorable for constructing wide bandgap D–A copolymer donors, and the multiple substitution positions allow to attach different functional groups for finely tuning the physicochemical properties of the polymers. For instance, the low-cost and high-performance Qx-based

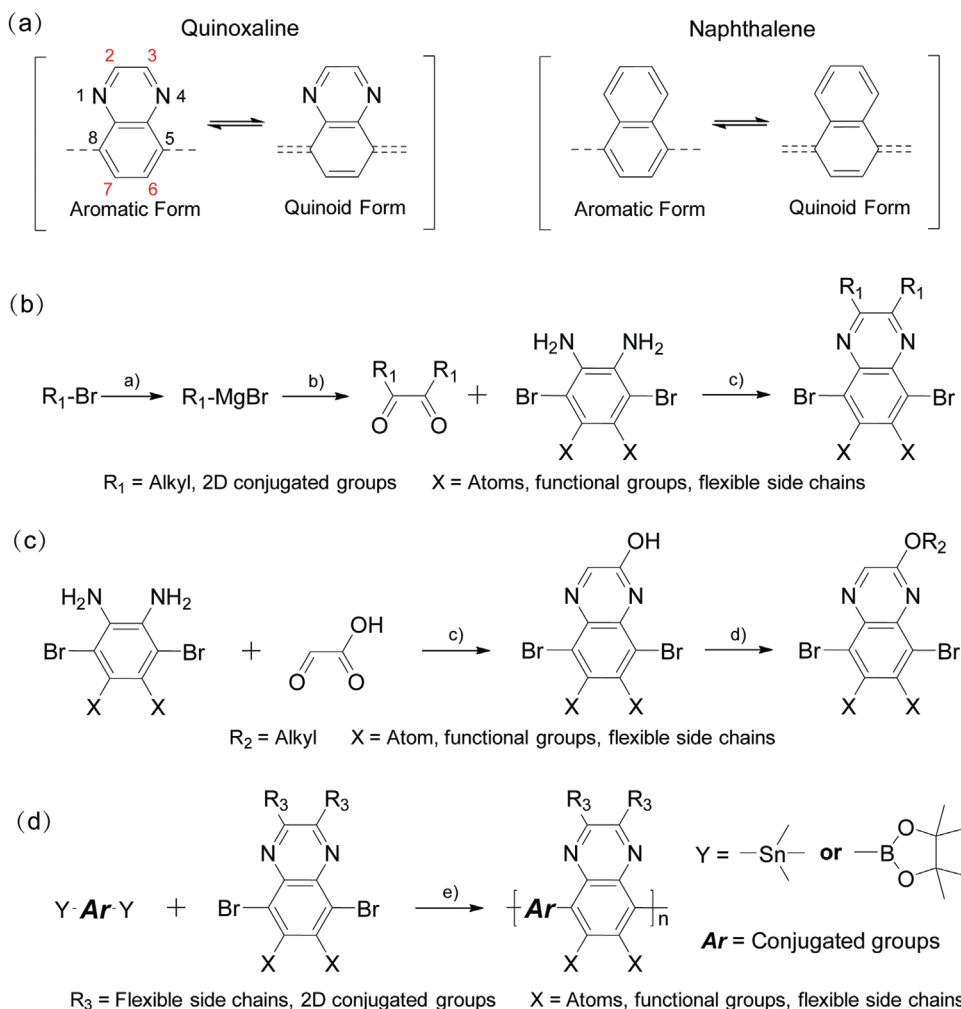
D–A copolymer PTQ11<sup>[21]</sup> was realized with two fluorine atoms substitution on 6, 7 positions for downshifting HOMO energy level and attaching an electron-donating alkyloxy and a methyl substituent on 2 and 3 positions, respectively, for enhancing absorbance of the polymer, benefiting from the multiple substitution positions of the Qx A-unit.<sup>[22–24]</sup> Thus, Qx unit and its derivatives are versatile and promising A-blocks for constructing the D–A copolymer photovoltaic molecules with diverse optoelectronic properties.

At early stage, researchers developed a lot of Qx-based D–A copolymer donors to match with the fullerene derivative acceptors for improving the photovoltaic performance of the PSCs,<sup>[25–33]</sup> which had pushed PCEs of the fullerene derivative-based PSCs to approach 10% in 2016.<sup>[34,35]</sup> Recently, the PSCs using the Qx-based D–A copolymers as donor and the A–DA'D–A structured narrow bandgap *n*-OS small molecule as acceptor achieved a high PCE of close to 18%.<sup>[36,37]</sup> Moreover, a series of low-cost and high-performance D–A copolymer donors (PTQ derivatives) based on thiophene D-unit and Qx A-unit have been developed recently, these PTQ derivatives shows high potential for industrial preparation and application.<sup>[21,38–41]</sup> In addition, the typical deep HOMO energy level of the Qx unit naturally leads to good stability of the corresponding D–A copolymers.<sup>[42]</sup> In general, high efficiency, low cost, and high stability of the photoactive molecules and the corresponding devices are the three crucial issues for the commercial application of the PSCs,<sup>[38]</sup> thus the Qx-based D–A copolymer donors are promising candidate for commercial application of the PSCs.

In this review, we summarized and discussed the recent development of the Qx-based D–A copolymer donors matching with the highly efficient narrow bandgap *n*-OS small molecule acceptors, aiming to better understand their molecular design strategies and structure–properties relationship for the high-performance polymer donors and PSCs. First, the common physicochemical properties and synthetic method of the Qx unit are presented. Second, the molecular design strategies of the Qx-based D–A copolymer donors, including backbone modulation, side chain optimization, and functional substitutions, are summarized and discussed with several representative copolymer examples. Then, a class of low-cost D–A copolymer donors (PTQ derivatives) based on thiophene D-unit and Qx A-unit are described and discussed. And, the Qx derivative-based D–A copolymer donors for the PSCs are also depicted subsequently. In addition, we also introduced the recent research progress of the Qx-based D–A copolymers for the application as hole transport material (HTM) in the perovskites, since the polymer hole transport material plays important role in improving stability of the perovskites. Finally, the perspectives, several fundamental challenges, and the outlooks of the Qx-based D–A copolymers are presented and discussed.

## 2. The Common Physicochemical Properties and Synthetic Method of the Qx Unit

Qx is a heterocyclic molecule which consists of two fused six-membered rings (benzene and pyrazine, thus Qx is also called benzopyrazine) with two N atoms distributed symmetrically in



**Scheme 1.** a) Aromatic and quinoid forms of the quinoxaline and naphthalene. b) Classic synthetic route of the Qx unit: a) Mg, THF; b) oxalyl chloride; c) acetic acid. c) Synthetic route of the Qx unit:<sup>[38]</sup> c) Acetic acid; d) *t*-BuOK, 1-bromoalkyl. d) Polymerization of the Qx-based D–A copolymers: e) Pd catalyst.

one of the rings (Scheme 1a).<sup>[20]</sup> The presence of two N atoms at the 1, 4 positions provides a weak electron-deficient characteristic of the Qx unit, thus it is an ideal A-unit to construct wide bandgap D–A copolymer donors by copolymerizing with various D-units. Moreover, the presence of two N atoms increases aromatic resonance energy of the Qx unit in comparison with its counterpart naphthalene, thus the Qx unit tends to favorably adopt a quinoid form through  $\pi$ -electrons delocalization. So, the Qx-based D–A copolymers possess shorter bond length and more obvious quinoid character along with the polymer backbone.<sup>[43]</sup> As the bandgap of conjugated polymers decreases linearly with increasing the quinoid character of the backbone, thus the Qx-based D–A copolymer donors could exhibit a relatively smaller bandgap. At the same time, the increased quinoid population in the conjugated polymers will induce an increased molecular coplanarity, which leads to enhanced intermolecular  $\pi$ - $\pi$  interactions in the film state. Therefore, the Qx-based D–A copolymers generally show ordered  $\pi$ - $\pi$  molecular stacking and thus high hole mobility in the film. Additionally, compared with other commonly used A-units (such as BT, BTz, BDD, etc.), Qx

unit has the unique superiority of easily modifiable molecular structure because of its more substitutable sites, as mentioned above. Thus, Qx unit is a versatile building block to construct the D–A copolymer donors with diverse and excellent optoelectronic properties.

The synthesis of the Qx unit was first reported through a condensation reaction between 1,2-diaminobenzene and glyoxal in 1884.<sup>[44]</sup> Since then until today, researchers have put a lot of efforts into the synthesis of Qx and its derivatives because of their diverse applications, aiming to invent new synthetic routes and to improve synthetic yield. The synthesis of the Qx unit and its derivatives for the D–A copolymer donors adopts a classic condensation reaction between an *o*-diamine compound and a  $\alpha$ -dicarbonyl compound (Scheme 1b). Considering the basic requirements of organic photovoltaic molecules, the Qx unit is usually connected to the D-unit through 5, 8 positions to form D–A conjugated system. Thus, the above *o*-diamine compounds are usually 1,2-phenylenediamine with the same or different substituents (X) at 4, 5 positions and two Br atoms at 3, 6 positions for the subsequent coupling reactions, where the

substituents (X) at 4, 5 positions are generally F atom, Cl atom, cyano (CN), or alkoxy. Considering the convenience of the synthetic reactions, the above  $\alpha$ -dicarbonyl compounds usually possess two identical  $R_1$  groups, where the  $R_1$  groups can be alkyl chain or 2D conjugated aromatic group. The  $\alpha$ -dicarbonyl compounds are prepared in advance before the condensation ring-closing reaction, thus the structure complexity of the  $R_1$  groups significantly affects the difficulty of the synthesis. The  $\alpha$ -dicarbonyl compounds are typically synthesized through nucleophilic reaction between Grignard reagents (such as alkylmagnesium bromide and arylmagnesium bromide) and oxalyl chloride. The brominated hydrocarbons (such as brominated alkanes and brominated aromatic hydrocarbons) are first treated with magnesium chips in tetrahydrofuran (THF) under argon (Ar) protection to form the Grignard reagents; then, the prepared Grignard reagents are transferred to another flask containing lithium bromide and cuprous bromide dispersed in THF under Ar protection; subsequently, oxalyl chloride is added dropwise into the above reaction mixture, which is separated and purified by silica gel chromatography to afford the  $\alpha$ -dicarbonyl compounds. Then, the *o*-diamine compounds and the  $\alpha$ -dicarbonyl compounds undergo condensation reaction in acetic acid to afford the target Qx unit.<sup>[25,30]</sup> Finally, the Qx-based D–A copolymer donors are synthesized through Stille coupling or Suzuki coupling polycondensation reactions between the dibromo compounds and distanno compounds or dioxaborolane compounds, respectively (Scheme 1d).

Recently, Sun et al. reported several novel Qx units with different substituents at the 2, 3 positions, and developed several wide bandgap D–A copolymer donors with simple molecular structures based on thiophene D-unit and the Qx A-units.<sup>[21,38,40]</sup> The synthesis of these Qx units adopt a novel synthetic route of condensation ring-closing at first and then alkoxylation (Scheme 1c), which is different from the reported classic synthetic route of the Qx unit (Scheme 1b). The *o*-diamine compounds (such as 3,6-dibromo-4,5-difluorobenzene-1,2-diamine) are first treated with glyoxylic acid in acetic acid to form Qx unit without side chains; then, the Qx unit reacts with brominated alkanes in the presence of base (such as *t*-BuOK and  $K_2CO_3$ ) to form the target Qx unit with alkoxy side chains.<sup>[21,38,40]</sup> These Qx units show high synthetic overall yield and low synthetic cost due to the short synthetic route, thus the resulting D–A copolymer donors possess low-cost advantage for industrial application.

### 3. The Qx-Based D–A Copolymer Donors for Polymer Solar Cells

As mentioned above, a highly efficient polymer donor, matching with the narrow bandgap acceptors, needs to possess a wide bandgap to have an absorption spectrum complementary with the acceptor, a low-lying HOMO energy level, high hole mobility, and good solubility in the processing solvent. To meet the requirements, large numbers of the Qx-based D–A copolymer donors are designed through delicate molecular structure optimizations of backbone modulation (main chain engineering) and side chain substitution with functional substituents (side chain engineering). In this section, we will

summarize and discuss the molecular design strategies of the Qx-based D–A copolymer donors from the aspects of backbone modulations, side chain optimizations, and functional substitutions with representative copolymer examples.

#### 3.1. Backbone Modulation of the Qx-Based D–A Copolymer Donors

Molecular backbone of the D–A copolymer donors determines the fundamental properties of the molecules, such as absorption spectra and electronic energy levels.<sup>[45]</sup> By incorporating various D-units with the Qx A-unit, researchers have developed numerous highly efficient D–A copolymer donors with quite different photovoltaic performance.<sup>[46–48]</sup> In addition, it is worth noting that the  $\pi$ -bridges (such as thiophene, selenophene, thieno[3,2-*b*]thiophene, etc.) are widely used between the D-units and the Qx A-unit to limit the steric hindrance and facilitate the  $\pi$ -conjugation along the backbone of the D–A copolymers.<sup>[49,50]</sup>

BDT unit is one of the most successful D-unit to build excellent D–A copolymer donors for PSCs due to its planar conjugated structure and suitable electronic property that makes it attractive for achieving highly tunable electronic energy levels and light absorption, as well as the high hole mobility of its D–A copolymers.<sup>[6]</sup> In 2016, Yuan et al. designed and synthesized two medium bandgap D–A copolymer donors (namely, PffQx-T and PffQx-PS; see **Figure 1**) based on the BDT D-unit, a bifluoroquinoxaline (ffQx) A-unit and thiophene  $\pi$ -bridges, for complementary light absorption with the narrow bandgap n-OS acceptor ITIC.<sup>[51]</sup> PffQx-T and PffQx-PS possess 2-ethylhexylthiophenyl and 4-ethylhexylthio-1-phenyl conjugated side chains on their BDT units, respectively. PffQx-PS exhibits deeper HOMO energy level (–5.40 eV, as shown in **Table 1**) than that (–5.36 eV) of PffQx-T due to the higher ionization potential of the benzene side chain of PffQx-PS than the thiophene side chain of PffQx-T. In addition, the formation of  $p_\pi(C)$ – $d_\pi(S)$  orbital overlap between benzene and the alkylthio chain in the conjugated side chains could also downshift the HOMO energy level of PffQx-PS. When using ITIC as acceptor, the PffQx-PS:ITIC-based blend film exhibits more suitable phase separation and bicontinuous interpenetrating network morphology, thus higher charge carrier mobilities than the PffQx-T:ITIC-based blend film. In addition, both devices based on PffQx-T:ITIC and PffQx-PS:ITIC can achieve efficient exciton dissociation even though the small HOMO energy level offset (0.12 eV for PffQx-T:ITIC pair and 0.08 eV for PffQx-PS:ITIC pair) between the donor and the acceptor. As a result, the PffQx-PS:ITIC-based PSC demonstrates a higher PCE of 9.12% with a higher  $V_{oc}$  of 0.97 V and a higher FF of 62.9% in comparison with that (PCE of 8.47% with a  $V_{oc}$  of 0.87 V and an FF of 59.6%) of the PffQx-T:ITIC-based PSC (Table 1). The higher  $V_{oc}$  of the PSC based on PffQx-PS:ITIC should be benefited from the lower-lying HOMO energy level of the PffQx-PS polymer donor.

In addition to the BDT unit, other electron-rich D-units are also used to construct the Qx-based D–A copolymer donors. For example, in 2018, Yang et al. reported a series of wide bandgap Qx-based D–A copolymer donors P1–P4 (Figure 1) by using benzene with different numbers of F atom substitution



**Table 1.** Optical properties, electronic energy levels, and photovoltaic performance parameters of the Qx-based D–A copolymer donors with backbone modulation.

Copolymer donor	$E_{opt}$ [eV]	HOMO [eV]	LUMO [eV]	$V_{oc}$ [V]	$J_{sc}$ [mA cm <sup>-2</sup> ]	FF [%]	PCE [%]	Acceptor	Refs.
PffQx-T	1.73	-5.36	-3.56	0.87	16.33	59.6	8.47	ITIC	[51]
PffQx-PS	1.81	-5.40	-3.55	0.97	14.96	62.9	9.12	ITIC	[51]
P1	1.87	-5.17	-2.90	0.86	8.53	66.22	4.86	IDIC	[52]
P2	1.90	-5.33	-2.94	0.91	13.15	64.84	7.75	IDIC	[52]
P3	1.92	-5.54	-2.98	1.00	15.99	60.89	9.70	IDIC	[52]
P4	2.00	-5.68	-3.13	1.06	4.82	57.43	2.93	IDIC	[52]
PQSeCz	1.67	-5.54	-3.68	/	/	/	/	/	[53]
PQSeFl	1.51	-5.58	-3.68	/	/	/	/	/	[53]
PPyQx <sub>ff</sub>	1.77	-5.47	-3.62	/	/	/	/	/	[54]
PPyQx	1.77	-5.41	-3.62	/	/	/	/	/	[54]
PIDT-QxM	1.83	-5.18	-3.15	0.74	20.78	61.0	9.49	Y6BO	[55]
PIDTT-QxM	1.82	-5.09	-3.15	0.73	23.25	61.3	10.40	Y6BO	[55]
PE64	1.70	-5.16	-3.53	0.50	14.05	50.0	3.54	Y6	[56]
PE65	1.71	-5.29	-3.50	0.77	25.20	67.0	13.01	Y6	[56]
PTBOQ	1.70	-5.36	-3.64	0.91	7.99	35.7	2.60	ITIC	[57]
PTBOQ-F	1.70	-5.48	-3.69	0.96	11.88	51.4	5.84	ITIC	[57]
PTBOQ-2F	1.75	-5.60	-3.64	1.00	5.01	34.4	1.73	ITIC	[57]
PTBTQ-F	1.73	-5.34	-3.66	0.89	7.86	44.0	3.08	ITIC	[57]
P(BDTo-TTFQ)	1.87	-5.24	-3.37	0.77	9.60	54.0	3.99	ITIC	[58]
P(BDtt-TTFQ)	1.84	-5.36	-3.52	0.84	14.06	57.0	6.69	ITIC	[58]
P(BDtsi-TTFQ)	1.85	-5.48	-3.63	0.95	11.61	57.0	6.21	ITIC	[58]

the mismatched HOMO energy level alignment between the donor and the acceptor.

In 2019, Yasa et al. developed two Qx-based D–A copolymer donors PQSeCz and PQSeFl (Figure 1) based on carbazole or fluorene as D-unit and selenophene as  $\pi$ -bridges.<sup>[53]</sup> Due to the lower ionization potential of selenophene, the introduction of selenophene  $\pi$ -bridges effectively downshifted the LUMO energy level of the polymers, which results in a reduced optical bandgap of the D–A copolymers. Therefore, PQSeCz and PQSeFl exhibit a narrow bandgap of 1.67 and 1.53 eV (Table 1), respectively. Then, Alqurashy et al. designed and synthesized two D–A copolymer donors PPyQx<sub>ff</sub> and PPyQx (Figure 1), consisting of pyrene as D-unit, Qx with or without F atom substitutions as A-unit, and bithiophene as  $\pi$ -bridges.<sup>[54]</sup> The polymers PPyQx<sub>ff</sub> and PPyQx exhibit similar physical properties with strong and broad absorbance from 400 to 700 nm and a similar optical bandgap of 1.77 eV (Table 1). The introduction of two F atoms to the Qx unit in the polymer PPyQx induces a downshifted HOMO energy level and the reduced  $\pi$ - $\pi$  stacking distance of the polymer. Recently, Wardani et al. reported two wide bandgap Qx-based D–A copolymer donors PIDT-QxM and PIDTT-QxM (Figure 1) by employing the indacenodithiophene (IDT) and indacenodithieno[3,2-*b*]thiophene (IDTT) as D-unit, respectively.<sup>[55]</sup> Thanks to the larger rigid plane of IDTT unit than IDT unit, the polymer PIDTT-QxM with IDTT D-unit shows higher extinction coefficient ( $\epsilon = 5.18 \times 10^{-4} \text{ M}^{-1} \text{ cm}^{-1}$ ) than that ( $\epsilon = 4.49 \times 10^{-4} \text{ M}^{-1} \text{ cm}^{-1}$ ) of the polymer PIDT-QxM with IDT D-unit. And the existence of more coplanar IDTT

D-unit in the polymer PIDTT-QxM significantly improves the formation of its molecular face-on orientation with respect to the surface, which facilitates the charge transport in the vertical direction. Therefore, the PIDTT-QxM-based device exhibits better photon harvest, charge separation, and transport than the PIDT-QxM-based device. As a result, the PIDTT-QxM:Y6BO-based PSC demonstrates a better photovoltaic performance (PCE = 10.40%,  $J_{sc} = 23.35 \text{ mA cm}^{-2}$ ) than the PIDT-QxM:Y6BO-based PSC (PCE = 9.49%,  $J_{sc} = 20.78 \text{ mA cm}^{-2}$ ) due to the significantly improved  $J_{sc}$  (Table 1).

Dithieno[2,3-*d*;2',3'-*d'*]benzo[1,2-*b*;4,5-*b'*]dithiophenes (DTBDT) unit, which has larger conjugated plane than BDT unit, is also one of the commonly used D-units for the D–A copolymers. In 2020, Zhou et al. reported two medium bandgap Qx-based D–A copolymer donors PE64 and PE65 (Figure 1) by using bithienyl DTBDT with (PE65) or without (PE64) Cl atom substitution on their thiophene conjugated side chain as D-unit, to study the impact of the introduced Cl atoms on the photovoltaic properties of the polymers.<sup>[56]</sup> The polymer PE65 shows a much deeper HOMO energy level of -5.29 eV (Table 1) due to the electron-withdrawing property of the Cl atom, which is beneficial for obtaining higher  $V_{oc}$ . Furthermore, chlorination of the thiophene conjugated side chain on DTBDT unit is beneficial to form face-on molecular orientation and favorable phase separation for the polymer PE65, which facilitates the charge transfer and reduces the charge carrier recombination to significantly improve the photovoltaic performance of the devices. Notably, the PE65-based PSC with *n*-OS Y6 as acceptor exhibits

a high PCE of 13.01% (Table 1) with simultaneously enhanced  $V_{oc}$ ,  $J_{sc}$  and FF in comparison with that (PCE = 3.54%) of the PE64:Y6-based PSC.

In addition to the above-mentioned binary D–A copolymer donors, researchers also developed ternary Qx-based D–A copolymer donors. In 2017, Wang et al. designed and synthesized a series of D–A1–D–A2 structured copolymer donors PTBOQ, PTBOQ-F, PTBOQ-2F, and PTBTQ-2F (Figure 1) by regularly alternating copolymerization of the simplest D-unit of thiophene, with the 2D conjugated Qx with or without fluorination as A1-unit and dialkoxy substituted benzoxadiazole (BO) or BT as A2-unit.<sup>[57]</sup> In these polymers, short flexible alkyl chains are distributed over the dual A-units to mitigate the steric hindrance while guarantee good solution processability of the polymers. The stronger electron-deficient feature of the BO unit can enhance the ICT effects, while the weaker electron-deficient feature of the Qx unit can strengthen the  $\pi$ – $\pi$  interactions through the favorable quinoidal form structure. In addition, F atom on the Qx unit further regulate the electronic structure, aggregation behavior, molecular packing feature, and charge transport ability of the donor materials. Finally, the polymer PTBOQ-F-based PSC with *n*-OS ITIC as acceptor exhibits a PCE of 5.84% (Table 1) with a  $J_{sc}$  of 11.88 mA cm<sup>-2</sup> and a FF of 51.4%.

In general, backbone modulation of the D–A copolymer donors is accompanied by the  $\pi$ -bridges optimization. For example, Tamilavan et al. introduced 3-hexylthiophene unit as additional  $\pi$ -bridges to the backbones of their D–A copolymer donors P(BDTo-TFQ), P(BDtt-TFQ), and P(BDTSi-TFQ), and reported three new D–A copolymer donors P(BDTo-TTFQ), P(BDtt-TTFQ), and P(BDTSi-TTFQ) (Figure 1).<sup>[58]</sup> This optimization leads to the upshifted HOMO energy levels and red-shifted absorption spectra of the resulting polymers. Moreover, all the three polymers with additional  $\pi$ -bridges show higher molecular coplanarity in comparison with their counterpart polymers. Thus, the three polymers (P(BDTo-TTFQ), P(BDtt-TTFQ), and P(BDTSi-TTFQ)) exhibit higher molecular crystallinity and greater hole mobility. Consequently, the polymers P(BDTo-TTFQ)- and P(BDtt-TTFQ)-based PSCs exhibit comparable PCEs (3.99% and 6.69% respectively, as shown in Table 1) to those of the polymers P(BDTo-TFQ)-based and P(BDtt-TFQ)-based (PCEs of 3.49% and 7.06%, respectively) PSCs when combined with *n*-OS acceptor ITIC, which should be mainly ascribed to a trade-off between the increased  $J_{sc}$  and the reduced  $V_{oc}$  of the devices. The PSC based on P(BDTSi-TFQ):ITIC shows a very low PCE of 0.75%, due to the mismatched HOMO energy levels of the donor and acceptor (the HOMO energy level (–5.58 eV) of the polymer donor P(BDTSi-TFQ) is lower than that (–5.50 eV) of the acceptor ITIC), thus the hole transfer from the acceptor to the donor is restricted. In contrast, the P(BDTSi-TTFQ):ITIC-based PSC exhibits a significantly improved PCE of 6.21% compared to the P(BDTSi-TFQ):ITIC-based PSC due to the upshifted HOMO energy level of P(BDTSi-TTFQ).

### 3.2. Side Chain Optimization of the Qx-Based D–A Copolymer Donors

The type and topological structure of side chains of the D–A copolymer donors significantly affects the molecular electronic

energy level, aggregation behavior, solubility, miscibility with electron acceptor, and intermolecular interactions (including the donor–donor interaction, donor–acceptor interaction, and acceptor–acceptor interaction), thus affecting the photovoltaic performance of the polymers.<sup>[59–61]</sup> Therefore, the systematic side chain engineering is crucial for obtaining high performance Qx-based D–A copolymer donors. The most commonly used side chains include alkyl, alkoxy, alkylthio, and 2D conjugated side chains, etc.

The side chain engineering of the Qx-based D–A copolymer donors can be divided into side chain optimizations of the D-units and the A-units of the polymers. Regarding the side chain optimization of the D-unit, the researches mainly focused on the optimization of BDT unit due to its excellent physicochemical properties. For example, in 2017, Wang et al. developed a novel BDT D-unit with a 2-(triisopropylsilyl)ethynyl thienyl conjugated side chain, and reported a medium bandgap Qx-based D–A copolymer donor PBdTSi-Qx (Figure 2) with thiophene as  $\pi$ -bridges.<sup>[62]</sup> PBdTSi-Qx shows an optical bandgap of 1.73 eV (Table 2) with the absorption edge located at 717 nm. The connection of triisopropylsilyl ethynyl group on the thiophene conjugated side chain of BDT unit not only lowers the HOMO energy level and extends the  $\pi$  conjugation plane of the polymer, but also promotes the intermolecular  $\pi$ – $\pi$  interactions. When combining the polymer donor PBdTSi-Qx with the *n*-OS acceptor ITIC, the corresponding PSC demonstrates a PCE of 4.38% with a  $V_{oc}$  of 0.91 V, a  $J_{sc}$  of 9.47 mA cm<sup>-2</sup>, and an FF of 50.9% (Table 2). In 2018, Li et al. designed and synthesized two medium bandgap Qx-based D–A copolymer donors *ff*Qx-TS1 and *ff*Qx-TS2 (Figure 2), based on two BDT D-units with different alkylthio side chains (branched 2-butyloctyl side chain for *ff*Qx-TS1 and straight dodecyl side chain for *ff*Qx-TS2), for investigating the influence of different alkylthio side chain on the photovoltaic performance of the corresponding PSCs.<sup>[63]</sup> Both polymers exhibit good solubility in common solvents and strong light absorption in the wavelength region of 300 to 700 nm. The *ff*Qx-TS2 film with straight alkylthio side chain delivers a smaller root-mean-square (RMS) roughness value of 0.86 nm than that (1.40 nm) of the *ff*Qx-TS1 film with branched alkylthio side chain. The lower RMS value benefits the ohmic contact between the photoactive layer and the interface layer, which helps to increase the  $J_{sc}$ . As a result, a higher PCE of 7.69% (Table 2) is obtained in the *ff*Qx-TS2-based PSC than that of the *ff*Qx-TS1-based device, due to its obviously enhanced  $J_{sc}$  (from 13.54 to 15.25 mA cm<sup>-2</sup>). In 2019, Tamilavan et al. reported three Qx-based D–A copolymer donors by side chain optimization of the BDT D-unit.<sup>[64]</sup> The three polymers are P(BDTo-TFQ) with 2-butyloctyloxy side chain, P(BDtt-TFQ) with 2-butyloctylthiophene side chain, and P(BDTSi-TFQ) with triisopropylsilyl ethynyl side chain on the BDT units, respectively (Figure 2). The HOMO energy levels of the three polymer donors are downshifted from –5.35 eV for P(BDTo-TFQ) with the alkyloxy side chain to –5.44 eV for P(BDtt-TFQ) with the thienyl conjugated side chain and to –5.58 eV for P(BDTSi-TFQ) with the alkylsilyl side chain. By using ITIC as acceptor with HOMO energy level of –5.50 eV, the P(BDtt-TFQ)-based PSC shows a higher PCE of 7.06% with a higher  $V_{oc}$  of 0.95 V than that of the P(BDTo-TFQ)-based PSC (Table 2), which should be ascribed to the deeper HOMO energy level and higher hole mobility of the polymer donor P(BDtt-TFQ).



**Table 2.** Optical properties, electronic energy levels, and photovoltaic performance parameters of the Qx-based D–A copolymer donors with side chain optimization.

Copolymer donor	E <sub>opt</sub> g [eV]	HOMO [eV]	LUMO [eV]	V <sub>oc</sub> [V]	J <sub>sc</sub> [mA cm <sup>-2</sup> ]	FF [%]	PCE [%]	Acceptor	Refs.
PBDTSi-Qx	1.73	-5.42	-2.95	0.91	9.47	50.9	4.38	ITIC	[62]
ffQx-TS1	1.77	-5.35	-3.51	0.93	13.54	55.0	6.94	ITIC	[63]
ffQx-TS2	1.73	-5.25	-3.49	0.91	15.25	56.0	7.69	ITIC	[63]
P(BDTSi-TFQ)	1.88	-5.35	-3.47	0.88	9.04	44.0	3.49	ITIC	[64]
P(BDTS-TFQ)	1.86	-5.44	-3.58	0.95	13.05	57.0	7.06	ITIC	[64]
P(BDTSi-TFQ)	1.94	-5.58	-3.64	0.92	2.31	35.0	0.75	ITIC	[64]
HFQx-T	1.76	-5.45	-3.50	0.92	15.59	65.0	9.40	ITIC	[65]
HFAQx-T	1.73	-5.50	-3.44	0.94	15.4	66.0	9.6	ITIC	[66]
TTFQx-T1	1.69	-5.31	-3.62	0.90	16.88	69.24	10.52	ITIC	[67]
TTFQx-T2	1.71	-5.38	-3.67	0.94	13.75	56.11	7.22	ITIC	[67]
TPQ-1	1.76	-5.26	-3.43	0.90	14.95	64.3	8.6	<i>o</i> -IDTBR	[68]
PBDTTS-TClQx	1.68	-5.35	-3.58	0.96	17.07	77.2	12.59	MeIC	[69]
PBDTTS-TClSQx	1.66	-5.43	-3.60	0.96	15.79	73.5	11.10	MeIC	[69]
PBQ7	1.79	-5.38	-3.14	0.81	25.83	64.3	13.45	Y6	[70]
PBQ10	1.92	-5.47	-2.89	0.85	25.77	74.6	16.34	Y6	[70]
PBQ5	1.88	-5.55	-2.91	0.84	26.02	70.81	15.55	Y6	[71]
PBQ6	1.71	-5.64	-3.18	0.85	26.58	77.91	17.62	Y6	[71]
PBDTT-EFQx	1.57	-5.41	-3.67	0.80	13.1	48.0	5.0	ITIC	[72]

Moreover, they designed and synthesized a new Qx A-unit by changing the alkoxy-substituted *m*-difluorobenzene conjugated side chain of the HFQx unit to the alkyl-substituted fluorothiophene conjugated side chain for finely tuning the photovoltaic properties of the polymer donor. Then, they synthesized two new D–A copolymer donors based on the Qx A-unit and BDT D-unit: TTFQx-T1 and TTFQx-T2 (Figure 2).<sup>[67]</sup> The polymer TTFQx-T1 with 2-ethylhexyl-thienyl conjugated side chain on BDT D-unit shows improved light absorption and hole mobility in comparison with the polymer TTFQx-T2 with 2-butyloctyl-thienyl conjugated side chain on BDT D-unit, due to its shorter alkyl side chain on the thienyl conjugated side chains. Moreover, the TTFQx-T1:ITIC blend film exhibits lower geminate recombination, clear nanoscale phase separation, suitable domain size, and higher charge carrier mobility than those of the TTFQx-T2:ITIC blend film. Therefore, the PSC based on TTFQx-T1:ITIC exhibits a higher PCE of 10.52% with V<sub>oc</sub> of 0.90 V, J<sub>sc</sub> of 16.88 mA cm<sup>-2</sup>, and FF of 69% (Table 2) than that of the TTFQx-T2:ITIC-based device (PCE of 7.22%, V<sub>oc</sub> of 0.94 V, J<sub>sc</sub> of 13.75 mA cm<sup>-2</sup>, and FF of 56%) due to the simultaneously improved J<sub>sc</sub> and FF. In addition, the inverted-structured PSC based on TTFQx-T1:ITIC with a large photoactive area of 16 mm<sup>2</sup> also demonstrates a higher PCE of 9.21%. In 2018, they further designed and synthesized a novel Qx-based D–A copolymer donor TPQ-1 (Figure 2) by employing an asymmetric Qx A-unit that contains two different conjugated side chain (alkylthiophene and alkoxybenzene) to regulate the molecular crystallinity.<sup>[68]</sup> Compared with its counterpart polymer HFQx-T that contains two identical alkoxy substituted *m*-difluorobenzene conjugated side chains, the polymer TPQ-1 shows reduced molecular crystallinity. When using a strong-crystalline *n*-OS *o*-IDTBR as acceptor, the PSC with TPQ-1 as donor exhibits a

favorable phase separation and microscopic morphology. While the HFQx-T:*o*-IDTBR blend films show excessive molecular self-aggregation, thus causing poor exciton dissociation. Consequently, the PSC based on the combination of weak-crystalline polymer TPQ-1 as donor and strong-crystalline *o*-IDTBR as acceptor demonstrates a higher PCE of 8.6% (Table 2) than that of the device based on the strong-crystalline polymer HFQx-T as donor and strong-crystalline *o*-IDTBR as acceptor. PCE of the TPQ-1-based device is further improved to 9.6% when a narrow bandgap D–A copolymer PTB7-Th is used as third component for morphology regulation of the photoactive layer.

In 2021, Zeng et al. developed two medium bandgap D–A copolymer donors PBDTTS-TClQx and PBDTTS-TClSQx (Figure 2) based on the Cl atom and alkyl or alkylthio substituted Qx as A-unit and alkylthio-thienyl substituted BDT as D-unit.<sup>[69]</sup> PBDTTS-TClQx with alkyl substituents on Qx A-unit displays strong light absorption in 500–750 nm region with a maximum molar absorption coefficient of 1.30 × 10<sup>5</sup> M<sup>-1</sup> cm<sup>-1</sup>, which is slightly higher than that of PBDTTS-TClSQx (1.18 × 10<sup>5</sup> M<sup>-1</sup> cm<sup>-1</sup>). After blending with the *n*-OS acceptor MeIC, the PBDTTS-TClQx:MeIC blend film exhibits more efficient exciton dissociation, less charge carrier recombination, more balanced electron/hole mobility ( $\mu_h/\mu_e$ ), and more preferred microscopic morphology in comparison with the PBDTTS-TClSQx:MeIC blend film. In consequence, the PBDTTS-TClQx:MeIC-based PSC shows a higher PCE of 12.59% (Table 2) than the device based on PBDTTS-TClSQx:MeIC with a PCE of 11.10%, which is benefited from the enhanced J<sub>sc</sub> of 17.07 mA cm<sup>-2</sup> and FF of 77.2% of the PBDTTS-TClQx-based device.

Recently, several highly efficient Qx-based D–A copolymer donors have been developed by side chain optimization of the

Qx unit, to match with the emerging *n*-OS acceptor Y6 and its derivatives. For instance, Sun et al. designed and synthesized a new D–A copolymer donor PBQ10 (Figure 2), by copolymerizing a 2D conjugated BDT D-unit and a bifluoroquinoxaline A-unit with monoalkoxy side chain to regulate the molecular electronic energy level and self-assembly feature.<sup>[70]</sup> In comparison with its counterpart copolymer PBQ7 with 2D conjugated dialkoxyphenyl side chain on its bifluoroquinoxaline A-unit, PBQ10 shows obviously downshifted HOMO energy level (−5.47 eV for PBQ10 vs −5.38 eV for PBQ7, as shown in Table 2) due to the relatively weaker electron-donating ability of monoalkoxy group compared to that of dialkoxyphenyl group. In addition, benefiting from the relatively smaller spatial conformation of monoalkoxy group, the polymer PBQ10 exhibits more preferential face-on molecular orientation, tighter  $\pi$ – $\pi$  stacking, higher molecular crystallinity, as well as higher hole mobility ( $5.22 \times 10^{-4} \text{ cm}^2 \text{ V}^{-1} \text{ s}^{-1}$  for PBQ10 vs  $1.71 \times 10^{-4} \text{ cm}^2 \text{ V}^{-1} \text{ s}^{-1}$  for PBQ7) than that of PBQ7. As a result, the PBQ10-based PSC with Y6 as acceptor demonstrates an impressive PCE of 16.34% (Table 2) with simultaneously increased  $V_{oc}$  of 0.85 V and FF of 74.6%, which is significantly higher than the PBQ7:Y6-based PSC (PCE of 13.45%,  $V_{oc}$  of 0.81 V and FF of 64.3%). Recently, Zhu et al. reported two new D–A copolymer donors, PBQ5 and PBQ6 (Figure 2), based on the 2D conjugated BDT as D-unit, difluoroquinoxaline (DFQ) with different side chains as A-unit, and thiophene as  $\pi$ -bridges.<sup>[71]</sup> The polymer PBQ6 based on the DFQ A-unit with two alkyl-substituted fluorothiophene side chains possesses red-shifted absorption spectrum, stronger intermolecular interaction, and higher hole mobility than the polymer PBQ5 based on the DFQ A-unit with two alkyl side chains. In addition, the PBQ6-based blend film with Y6 as acceptor shows higher and balanced hole/electron mobilities, less charge carrier recombination, longer charge carrier lifetime, and more favorable aggregation morphology than that of the PBQ5:Y6-based blend film. Therefore, the PSC based on PBQ6:Y6 achieves a PCE as high as 17.62% (Table 2) with a high FF of 77.91%, which is significantly higher than the PCE (15.55%) of the PBQ5:Y6-based PSC. Indeed, the PCE of 17.62% is one of the highest efficiencies for the binary PSCs, which indicates the great potential of the Qx-based D–A copolymer donors for high-performance PSCs.

In addition, the side chains with strong electron-withdrawing characteristic are also used to regulate the molecular photovoltaic properties. In 2020, Luo et al. reported a novel Qx (EFQx) unit with two ester side chain, and synthesized a new D–A copolymer donor PBDTT-EFQx (Figure 2) based on the EFQx A-unit and the 2D conjugated BDT D-unit.<sup>[72]</sup> The polymer PBDTT-EFQx shows a narrow optical bandgap of 1.57 eV (Table 2) with absorption edge located at 790 nm due to the strong ICT effect between the BDT electron-rich unit and the Qx electron-deficient unit. And the polymer PBDTT-EFQx presents appropriate energy level alignment with the commonly used *n*-OS electron acceptors (such as small molecule acceptor ITIC and polymer acceptor N2200). However, the PBDTT-EFQx:ITIC-based PSC and the PBDTT-EFQx:N2200-based PSC only demonstrate a moderate PCE of 5.0% and 4.1% (Table 2) respectively, which is ascribed to the overlapping absorption spectra of electron donor and electron acceptor. Despite the moderate photovoltaic performance of the polymer

PBDTT-EFQx, it reveals that the ester-substituted Qx unit is a potential building block for developing narrow bandgap D–A copolymer donors.

### 3.3. Functional Substitution of the Qx-Based D–A Copolymer Donors

Functional substitution (including electron-donating groups substitution and electron-withdrawing groups substitution) is another effective method to regulate the molecular photovoltaic properties, especially to regulate the molecular electronic structure and aggregation feature. In order to achieve higher PCEs, functional substitution of the Qx-based D–A copolymer donors is mainly by the electron-withdrawing groups to downshift the HOMO energy levels of the polymers for higher  $V_{oc}$ . Over the past few years, several electron-withdrawing groups, such as F atom, Cl atom, cyano, and ester, are employed to modify the molecular structures of the Qx-based D–A copolymer donors for desired properties.<sup>[73–75]</sup>

Halogenation (especially fluorination and chlorination) of the D–A copolymer donors has proven its validity on molecular structure optimization. In 2016, Zou and co-workers reported a medium bandgap D–A copolymer donors PffQx-T (Figure 3), and an efficient PSC based on the PffQx-T:ITIC with a PCE of 8.47% ( $V_{oc}$  of 0.87 V,  $J_{sc}$  of  $16.33 \text{ mA cm}^{-2}$ , and FF of 59.6%, as shown in Table 3).<sup>[51]</sup> To further modify the photovoltaic properties of the PffQx-T polymer donor, in 2017, they introduced additional two F atoms to the phenyl conjugated side chain of the Qx unit of PffQx-T, and synthesized a hexafluoro-substituted quinoxaline (HFQx) unit and a medium bandgap D–A copolymer donor HFQx-T<sup>[65]</sup> (Figure 3). The strong electron-withdrawing properties of the six F atoms dramatically downshift the HOMO energy level of the polymer HFQx-T to −5.45 eV (Table 3). In addition, F atoms enhance the absorption coefficient of the polymer and modify the blend film morphology. As a result, the HFQx-T:ITIC-based device achieves an impressive PCE of 9.4% (Table 3) with a higher  $V_{oc}$  of 0.92 V, a large  $J_{sc}$  of  $15.60 \text{ mA cm}^{-2}$ , and a higher FF of 65%.

In 2017, Zheng et al. developed three Qx-based D–A copolymer donors, PBQ-0F, PBQ-QF, and PBQ-4F (Figure 3), based on the 2D conjugated BDT with or without fluorine substitution as D-unit, Qx with or without fluorine-substitution as A-unit, and thiophene as  $\pi$ -bridges.<sup>[76]</sup> By introducing F atoms to the BDT unit and Qx unit, the frontier molecular orbital energy levels of the polymers are manipulated. The polymer PBQ-0F without F substitution has the highest LUMO and HOMO energy levels, while the polymer PBQ-4F with F atoms on both BDT unit and Qx unit shows the lowest LUMO and HOMO energy levels. In addition, the three polymers show similar scattering profiles with preferred face-on packing and nearly identical laminar and  $\pi$ – $\pi$  stacking peaks, indicating that fluorination of the polymers barely affects the molecular packing features. However, the different molecular packing features were observed when blending them with an *n*-OS acceptor ITIC. The PBQ-4F:ITIC blend film exhibits larger integrated  $\pi$ – $\pi$  intensity and thus has the most beneficial molecular packing than the other two blends. Thus, the PBQ-4F:ITIC blend film shows both highest hole mobility and highest electron mobility.

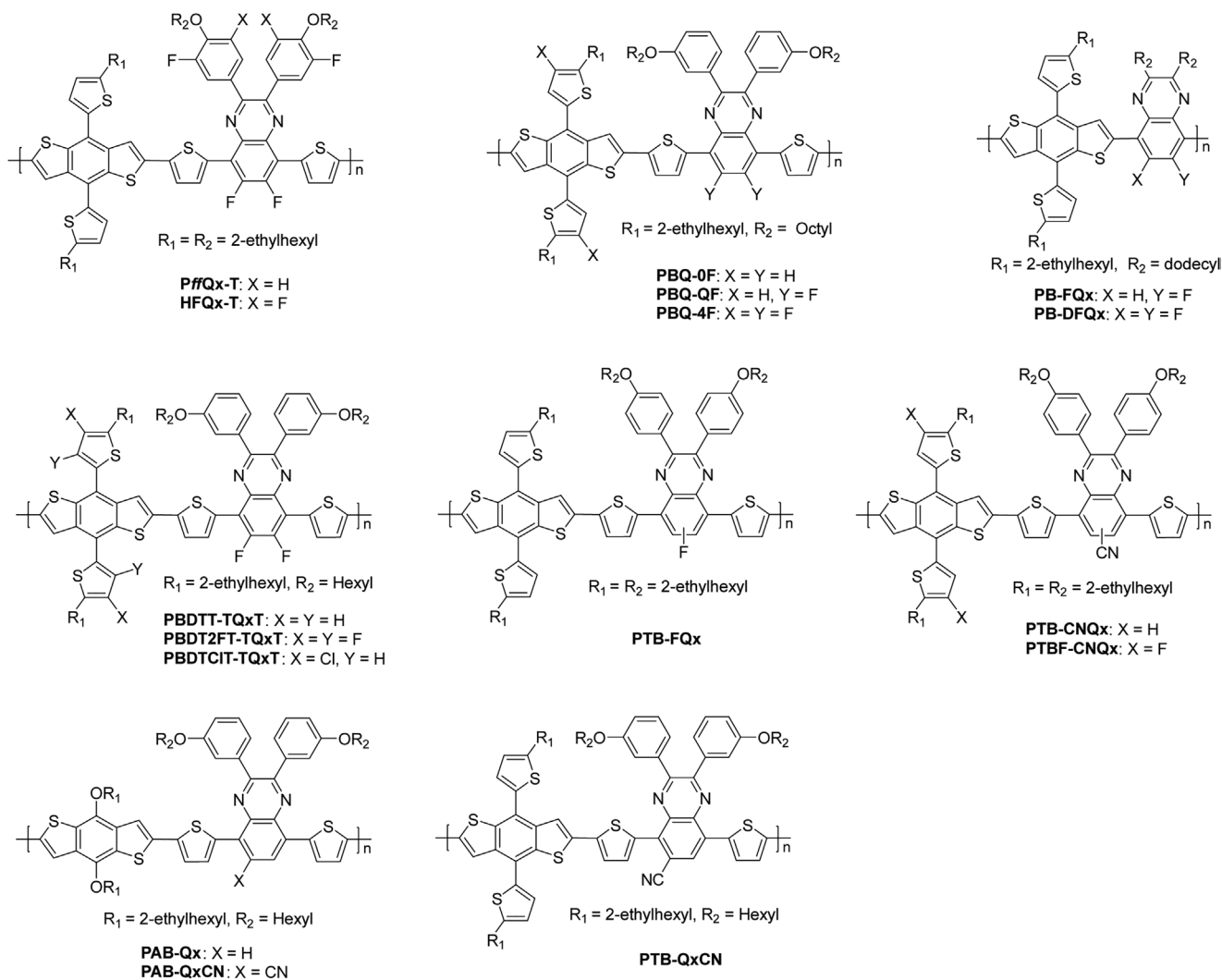


**Figure 3.** Molecular structures of the Qx-based D–A copolymers with functional substitution.

Consequently, the PBQ-4F:ITIC-based PSC achieves the highest PCE of 11.34% (Table 3) among the three polymer donors, resulted from the simultaneously improved  $V_{oc}$  of 0.95 V,  $J_{sc}$  of  $17.87 \text{ mA cm}^{-2}$ , and FF of 66.80%.

Recently, Keum et al. designed and synthesized two wide bandgap D–A copolymer donors PB-FQx and PB-DFQx (Figure 3) by directly copolymerizing a 2D conjugated BDT D-unit and a monofluoroquinoxaline (FQx) or a difluoroquinoxaline (DFQx) A-unit without the utilization of  $\pi$ -bridges.<sup>[77]</sup> Both polymers exhibit satisfactory thermal stability and broad light absorption band from 300 to 650 nm. And the HOMO energy levels of the polymers downshift with increasing the number of F atoms on the Qx unit, thus the polymer PB-DFQx shows a deeper HOMO energy level of  $-5.70 \text{ eV}$  (Table 3) than the polymer PB-FQx ( $-5.62 \text{ eV}$ ), which can lead to higher  $V_{oc}$  of the corresponding device. Finally, the PB-DFQx:ITIC-based PSC demonstrated a higher PCE of 6.31% with a higher  $V_{oc}$  of 0.99 V than that of the PB-FQx-based device (Table 3). Lenaerts et al. developed three D–A copolymer donors based on BDT with thienyl conjugated side

chains as D-units and a difluorinated Qx as A-unit, including PBDTT-TQxT with the thienyl substituents without halogenation, PBDT2FT-TQxT with the bifluoro-thienyl substituents and PBDTCIT-TQxT with the chloro-thienyl substituents on the BDT D-units (Figure 3), to investigate the impact of halogenation on the photovoltaic properties of the polymers.<sup>[78]</sup> The higher degree of halogenation in PBDT2FT-TQxT leads to the deeper HOMO energy level of the polymer, and the two F atoms on thiophene conjugated side chain cause a large twisted dihedral angle between the BDT center and the lateral thiophene side chains for the polymer PBDT2FT-TQxT. While, the excessive twist is avoided in the polymer PBDTCIT-TQxT with chlorine substitution. With using ITIC as acceptor, the PBDTCIT-TQxT-based PSC demonstrates the highest PCE of 8.43% as well as the higher  $V_{oc}$  (Table 3) because of the balanced charge carrier mobilities and favorable donor–acceptor interactions, while the PBDT2FT-TQxT-based PSC exhibits the lowest PCE (5.13%). The result suggests that rational halogenation of the D–A copolymer donors can improve their photovoltaic performance.

**Table 3.** Optical properties, electronic energy levels, and photovoltaic performance parameters of the Qx-based D–A copolymer donors with functional substitution.

Copolymer donor	E <sub>opt</sub> g [eV]	HOMO [eV]	LUMO [eV]	V <sub>oc</sub> [V]	J <sub>sc</sub> [mA cm <sup>-2</sup> ]	FF [%]	PCE [%]	Acceptor	Refs.
PfFQx-T	1.73	-5.36	-3.56	0.87	16.33	59.6	8.47	ITIC	[51]
HFQx-T	1.76	-5.45	-3.50	0.92	15.59	65.0	9.40	ITIC	[65]
PBQ-0F	1.70	-5.18	-3.48	0.69	16.16	59.91	6.68	ITIC	[76]
PBQ-QF	1.72	-5.34	-3.62	0.83	17.16	62.49	8.90	ITIC	[76]
PBQ-4F	1.79	-5.49	-3.70	0.95	17.87	66.80	11.34	ITIC	[76]
PB-FQx	1.84	-5.62	-3.64	0.98	10.30	58.0	5.83	ITIC	[77]
PB-DFQx	1.87	-5.70	-3.67	0.99	10.61	60.0	6.31	ITIC	[77]
PBDTT-TQxT	1.71	-5.46	-3.35	0.84	13.57	65.0	7.45	ITIC	[78]
PBDT2FT-TQxT	1.79	-5.58	-3.37	0.98	9.46	53.0	5.13	ITIC	[78]
PBDTCIT-TQxT	1.78	-5.53	-3.35	0.94	14.61	60.0	8.43	ITIC	[78]
PTB-FQx	1.72	-5.18	-3.46	0.63	23.5	50.2	7.4	Y6BO	[79]
PTB-CNQx	1.65	-5.33	-3.68	0.77	25.4	60.0	11.7	Y6BO	[79]
PTBF-CNQx	1.67	-5.48	-3.81	0.83	27.6	61.2	14.0	Y6BO	[79]
PAB-Qx	1.74	-5.37	-3.38	0.62	17.2	40.6	4.35	Y6BO	[80]
PAB-QxCN	1.64	-5.44	-3.48	0.78	22.5	59.7	8.66	Y6BO	[80]
PTB-QxCN	1.58	-5.39	-3.49	0.76	27.9	62.6	13.3	Y6BO	[80]

In addition to the halogenation, CN is often used as functional group to finely tune the optoelectronic properties of the D–A copolymers due to its strong electron-withdrawing feature. In 2020, Handoko et al. developed several CN-functionalized Qx-based D–A copolymer donors PTB-FQx, PTB-CNQx, and PTBF-CNQx (Figure 3) to investigate the effect of CN substituents on the photovoltaic properties of the polymers.<sup>[79]</sup> Compared to the reference polymer PTB-FQx with F atom on the Qx A-unit, the polymer PTB-CNQx with CN group on the Qx A-unit exhibits deeper HOMO energy level, stronger ICT interactions, and larger extinction coefficient due to the stronger electron-withdrawing ability of CN group than F atom. And these features are further enhanced in the polymer PTBF-CNQx with introducing additional F atoms to the BDT D-unit. Moreover, the consecutive introduction of CN group and F atom to the Qx A-unit and BDT D-unit of the polymer gradually improves the molecular face-on orientation relative to the surface. These favorable changes improve the charge generation and charge transport, and restrain the charge recombination characteristics of the devices with the *n*-OS Y6BO as acceptor, which leads to the simultaneously enhanced V<sub>oc</sub>, J<sub>sc</sub>, and FF of the PSCs. As a result, the PTBF-CNQx:Y6BO-based PSC demonstrates the highest PCE of 14.0% with the highest V<sub>oc</sub> of 0.83 V, the highest J<sub>sc</sub> of 27.6 mA cm<sup>-2</sup>, and the highest FF of 61.2% among the three polymer donors (Table 3). Recently, Sagita et al. reported a series of Qx-based D–A copolymer donors PAB-Qx, PAB-CNQx, and PTB-CNQx (Figure 3) with CN group on the Qx A-unit to elucidate the effect of strong electron-withdrawing CN groups on the photovoltaic properties of the polymers.<sup>[80]</sup> Compared to the control polymer PAB-Qx without CN group, the polymer PAB-CNQx with CN substituent shows downshifted HOMO energy level, enhanced light absorption, and increased charge carrier mobility. Moreover, the PAB-CNQx-based device with *n*-OS Y6BO as acceptor exhibits more efficient exciton

generation and separation with less charge recombination compared to the PAB-Qx:Y6BO-based device. Therefore, the PAB-CNQx:Y6BO-based device shows a significantly improved PCE of 8.66% (Table 3) with simultaneously increased V<sub>oc</sub>, J<sub>sc</sub>, and FF. Furthermore, the polymer PTB-CNQx with alkylthienyl conjugated side chain on BDT D-unit and CN substituent on Qx A-unit shows further enhanced light absorption,  $\pi$ – $\pi$  molecular stacking, and hole transport capability in comparison with the polymer PAB-CNQx. Consequently, PCE of the PTB-CNQx:Y6BO-based PSC increases to 13.3% with a higher J<sub>sc</sub> of 27.9 mA cm<sup>-2</sup> and a higher FF of 62.6% (Table 3).

### 3.4. The Low-Cost Qx-Based D–A Copolymer Donors

The application of PSCs requires the realization of high efficiency, low cost, and high stability simultaneously.<sup>[38]</sup> Due to the great innovations on developing highly efficient photovoltaic materials, PCE of the optimal single junction PSC has reached over 18% recently,<sup>[81]</sup> which has met the photovoltaic efficiency requirement for commercial application. However, synthetic cost of the most efficient photovoltaic materials are too high to achieve commercial application for the PSCs due to their complicated molecular structures, verbose multisteps synthesis, low synthetic yield, and multiple purifications.

To address this issue, in 2018, Sun et al. designed and synthesized a low-cost and high-performance D–A copolymer donor PTQ10 (Figure 4), by employing thiophene as D-unit and alkoxy substituted difluoroquinoxaline as A-unit without using  $\pi$ -bridges.<sup>[38]</sup> The alkoxy side chain on Qx unit is to enhance light absorption and to ensure good solubility of the polymer, while two F atoms on the Qx unit are for downshifting the HOMO energy level and increasing hole mobility of the polymer. PTQ10 possesses a simple molecular structure and

can be synthesized with high overall yield of 87.4% via only two-step chemical reactions from cheap raw materials, showing extremely high synthetic accessibility and low synthetic cost. Encouragingly, the PSC based on PTQ10 as donor and IDIC as acceptor demonstrates an impressive PCE of 12.70% (Table 4), which is one of the highest PCEs when the result was published. Moreover, photovoltaic performance of the PTQ10:IDIC-based device exhibits insensitivity of photoactive layer thickness from 100 to 300 nm, which is conducive to the large area fabrication of the devices. In addition, by using Y6 as acceptor, the PCE of the PTQ10-based PSC reached 16.53%.<sup>[39]</sup>

Then, they designed and synthesized four low-cost PTQ derivative donors (PTQ7, PTQ8, PTQ9, and PTQ10, as shown in Figure 4) with different fluorine substitution positions, to investigate the effect of fluorination forms on charge separation and open circuit voltage loss ( $V_{\text{loss}}$ ) of the PSCs with the PTQ derivatives as donor.<sup>[40]</sup> In comparison with the polymer PTQ7 without fluorination, the fluorinated polymers PTQ9 and PTQ10 show gradually downshifted HOMO energy levels with increasing the number of F atoms on Qx unit, which can help to obtain higher  $V_{\text{oc}}$ . The PSCs based on PTQ9:Y6 and PTQ10:Y6 show gradually enhanced charge separation, and gradually reduced  $V_{\text{loss}}$  due to the gradually reduced nonradiative recombination loss in comparison with the PTQ7:Y6-based PSC. Consequently, the PTQ10:Y6-based PSC demonstrates a high PCE of 16.21% (Table 4) with a low  $V_{\text{loss}}$  of 0.549 V and a low nonradiative recombination loss of 0.23 eV. While the polymer PTQ8 with two F atoms on its thiophene D-unit exhibits the deepest HOMO energy level of  $-5.68$  eV, which is beneficial to obtain highest  $V_{\text{oc}}$  (Table 4). However, the PTQ8-based PSC with *n*-OS Y6 as acceptor demonstrates the lowest PCE of 0.90% because of the extremely poor charge separation in the device, due to the mismatched HOMO energy levels alignment between the donor and acceptor (too low HOMO energy level of the polymer donor). The results indicate that fluorination on the Qx A-unit is important for the D–A copolymer donors, which can effectively suppress the nonradiative recombination loss, reduce  $V_{\text{loss}}$ , and achieve high photovoltaic performance of the corresponding PSCs. After that, several high-efficiency PSCs are reported by using the polymer PTQ10 as electron donor. For instance, Qin et al. reported a nonhalogen solvent processed tandem PSC with PTQ10 as polymer donor of its front cell, and the PCE of the tandem PSC reached 16.67%.<sup>[82]</sup> Chai et al. reported a PTQ10-based PSC with an impressive PCE of 17.7% (Table 4) by using a Y6 derivative acceptor with side chain modification, which is one of the highest PCEs of the single junction PSCs currently.<sup>[37]</sup> All these results indicate the great potential of PTQ10 as polymer donor for the commercial application of

PSCs, in considering its dual advantages of low cost and excellent photovoltaic performance.

In 2020, Sun et al. further introduced a methyl substituent onto the Qx A-unit of PTQ10, and reported a new low-cost and high-performance D–A copolymer donor PTQ11 (Figure 4).<sup>[21]</sup> Considering the weak electron-donating property of the methyl, PTQ11 exhibits a slightly upshifted HOMO energy level ( $-5.52$  eV, as shown in Table 4) than PTQ10 ( $-5.55$  eV). In addition, the introduction of methyl substituent induces an enhanced  $\pi$ – $\pi$  molecular stacking and molecular crystallization, thus PTQ11 shows better hole transport capability than PTQ10. When combined with an *n*-OS acceptor TPT10, which is the derivative of Y6 with monobromine instead of bifluorine substitution on its end groups, the PTQ11-based PSC shows highly efficient exciton dissociation and hole transfer, despite the zero HOMO energy level offset between the donor PTQ11 and the acceptor TPT10. As a result, the PTQ11:TPT10-based PSC demonstrates a high PCE of 16.32% (Table 4) with a  $V_{\text{oc}}$  of 0.88 V, a  $J_{\text{sc}}$  of  $24.79$  mA cm<sup>-2</sup>, and an FF of 74.8%. The result proves the feasibility of efficient hole transfer from the A–DA'D–A structured acceptor to the Qx-based D–A copolymer donor in the photoactive layer with zero donor/acceptor HOMO energy level offset.

In 2020, Yuan et al. developed several random ternary D–A copolymer donors (PQSi05, PQSi10, and PQSi25, as shown in Figure 4) with the same molecular backbone but different side chains (with partial siloxane-alkoxy side chain) on the Qx A-units in comparison with PTQ10, for modifying the optoelectronic properties of the polymers.<sup>[41]</sup> It is found that the polymers show enhanced molecular aggregation feature and reduced film surface energy with increasing the content of the siloxane-alkoxy side chain, which weakens the miscibility of the polymers with the electron acceptor. Finally, a maximum PCE of 13.56% (Table 4) is achieved in the PQSi05:IT-4F-based PSC with a  $V_{\text{oc}}$  of 0.911 V, a  $J_{\text{sc}}$  of  $21.42$  mA cm<sup>-2</sup>, and an FF of 69.48%.

### 3.5. The D–A Copolymer Donors Based on Qx Derivative as A-Unit

In addition to the subtle molecular structure optimization of the Qx-based D–A copolymer donors by the functionilations on D-unit and Qx A-unit, the D–A copolymer donors based on Qx derivatives as A-unit were also developed for high-performance PSCs.<sup>[27,83,84]</sup> For example, in 2017, Yu et al. reported two wide bandgap D–A copolymer donors PBDT-NQx and PBDTS-NQx (Figure 5) based on a quinoxalino[6,5-*f*]quinoxaline (NQx)

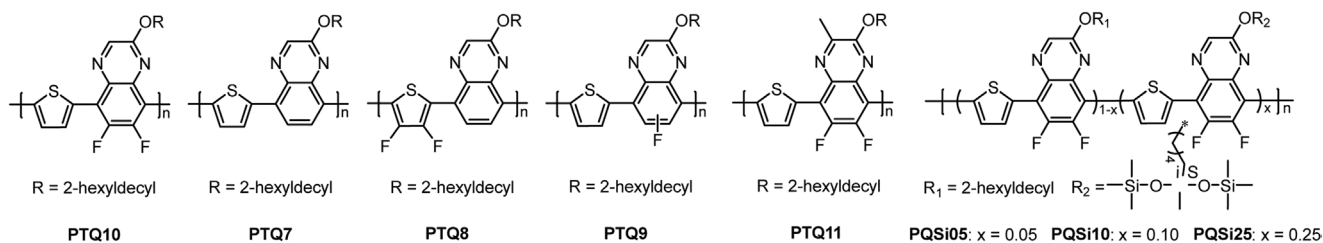


Figure 4. Molecular structures of the low-cost and high-performance Qx-based D–A copolymers (PTQ derivatives).

**Table 4.** Optical properties, electronic energy levels, and photovoltaic performance parameters of the low-cost and high-performance Qx-based D–A copolymer (PTQ derivatives) donors.

Copolymer donor	$E_{opt}$ [eV]	HOMO [eV]	LUMO [eV]	$V_{oc}$ [V]	$J_{sc}$ [ $\text{mA cm}^{-2}$ ]	FF [%]	PCE [%]	Acceptor	Refs.
PTQ10	1.92	−5.54	−2.98	0.97	17.81	73.6	12.7	IDIC	[38]
PTQ10	1.92	−5.54	−2.98	0.82	26.65	75.1	16.53	Y6	[39]
PTQ7	1.87	−5.38	−2.82	0.71	18.65	43.4	5.75	Y6	[40]
PTQ8	2.00	−5.68	−2.92	0.89	3.11	32.5	0.90	Y6	[40]
PTQ9	1.87	−5.41	−2.87	0.82	23.72	54.0	10.50	Y6	[40]
PTQ10	1.92	−5.55	−2.90	0.87	24.81	75.1	16.21	Y6	[40]
PTQ10	1.92	−5.55	−2.90	0.99	16.67	73.42	12.14	<i>m</i> -DTC-2Cl	[82]
PTQ10	1.92	−5.53	−2.81	0.88	25.3	79.3	17.7	<i>m</i> -BTP-C6Ph	[37]
PTQ10	1.92	−5.55	−2.90	0.92	17.25	58.2	9.24	TPT10	[21]
PTQ11	1.95	−5.52	−2.76	0.88	24.79	74.8	16.32	TPT10	[21]
PQSi05	1.93	−5.67	−3.74	0.91	21.42	69.48	13.56	IT-4F	[41]
PQSi10	1.92	−5.62	−3.71	0.91	21.12	69.28	13.32	IT-4F	[41]
PQSi25	1.92	−5.61	−3.69	0.89	21.07	69.75	13.10	IT-4F	[41]

A-unit, where two 2D conjugated BDT with alkyl or alkylthio substituted thiophene side chains are used as D-units for regulating photovoltaic properties of the polymers.<sup>[85]</sup> The attached 2D conjugated octylthienyl side chains on the NQx unit improves the  $\pi$ – $\pi^*$  transitions and the light absorptions of the polymers, thus both polymers exhibit strong absorption intensity from 300 to 700 nm. In comparison with PBDT-NQx with alkyl side chain on the 2D conjugated BDT unit, the alkylthio substituent induces a downshifted HOMO energy level of −5.31 eV for PBDTS-NQx (Table 5). In addition, the alkylthio substituent also enhances the molecular crystallinity of PBDTS-NQx, which is beneficial for boosting  $J_{sc}$  and FF of the resulting devices. Finally, the PBDTS-NQx-based PSC using ITIC as acceptor demonstrates a higher PCE of 11.47% with simultaneously enhanced  $V_{oc}$  of 0.92 V,  $J_{sc}$  of 17.86  $\text{mA cm}^{-2}$ , and FF of 69.8% than that (PCE = 9.11%,  $V_{oc}$  = 0.87 V,  $J_{sc}$  = 16.21  $\text{mA cm}^{-2}$ , and FF = 64.6%) of the PBDT-NQx:ITIC-based PSC (Table 5). In 2019, Huang and co-workers also developed a NQx-based D–A copolymer donor, PNQX-2F2T (Figure 5), through copolymerizing difluoro-substituted bithiophene (2F2T) D-unit and NQx A-unit.<sup>[86]</sup> The smaller size of the 2F2T unit without bulky chains allows for the closer alkyl-alkyl interdigitation and more ordered interchain lamellar stacking for the polymer PNQX-2F2T. In addition, the two F atoms on 2F2T unit can not only deepen the HOMO energy level of the polymer, but also enhance the noncovalent H...F and/or S...F interactions, which could lead to higher  $V_{oc}$  of the corresponding device, and improve the backbone coplanarity and molecular crystallinity of the polymer. When combined with a light absorption-complementary *n*-OS acceptor IT-M, the PNQX-2F2T-based PSC demonstrates a PCE of 7.5% (Table 5). In addition, they designed and synthesized several D–A copolymer donors (PDCB-Q812, PDCB-DFQ812, PDCB-Q1014, and PDCB-DFQ1014, as shown in Figure 5) based on a Qx derivative with or without fluorination as A-unit, the dicyanodistyrylbenzene as D-unit, and thiophene or alkyl substituted thiophene as  $\pi$ -bridges, to investigate the impact of fluorination and alkyl chains on photoelectric properties of the polymers.<sup>[87]</sup> It is found that different alkyl chains on

the thiophene  $\pi$ -bridges has little effect on the electronic energy levels while a moderate effect on the absorption coefficients of the polymers. In addition, the fluorinated polymers show not only deeper HOMO energy levels but also enhanced absorption coefficients and higher charge carrier mobilities than their non-fluorinated analogues, which is beneficial for obtaining higher  $V_{oc}$ ,  $J_{sc}$  and FF. As a result, by using the narrow bandgap *n*-OS ITIC as acceptor, the PSCs based on PDCB-DFQ812 and PDCB-DFQ1014 achieved higher PCE of 8.37% and 7.13%, respectively, with a high  $V_{oc}$  of over 1 V (Table 5).

In 2019, Zhang et al. designed and synthesized two thiophene-fused quinoxaline (QXT) units with different number of F atom on their alkylthienyl conjugated side chain, and reported two D–A copolymer donors (PBDTT-QXT-TF1 and PBDTT-QXT-TF2, as shown in Figure 5) by using QXT as the A-unit, 2D conjugated BDT as the D-unit, and thiophene as the  $\pi$ -bridges.<sup>[88]</sup> It is found that the fusion of a thiophene ring onto Qx unit results in a red-shifted absorption spectrum through stabilizing the quinoid structure of the conjugated backbone. However, the introduction of fused thiophene ring results in the increased molecular backbone twist, thus attenuating the ICT effect and light absorption intensity of the polymer, which results in the decrement of the  $J_{sc}$  for the corresponding PSCs. On the other hand, both the introduction of carboxyl group to the fused thiophene and fluorination of the alkylthienyl conjugated side chains downshift the HOMO energy level of the polymers, which is favorable for the increment of  $V_{oc}$ . As a result, the PSCs based on PBDTT-QXT-TF1 or PBDTT-QXT-TF2 as donor with IDIC as acceptor show higher  $V_{oc}$  but lower  $J_{sc}$ . The PBDTT-QXT-TF1:IDIC-based PSC exhibits a slightly higher PCE of 6.67% with  $V_{oc}$  of 0.951 V,  $J_{sc}$  of 11.56  $\text{mA cm}^{-2}$ , and FF of 60.65%, while the PBDTT-QXT-TF2:IDIC-based PSC shows a decreased PCE of 5.12% ( $V_{oc}$  of 0.975 V,  $J_{sc}$  of 9.78  $\text{mA cm}^{-2}$ , and FF of 53.61%) (Table 5).

Recently, Xu et al. designed and synthesized a Qx derivative, namely, dithieno[3,2-*f*:2',3'-*h*]quinoxaline (DTQx), by fusing two thiophene rings with Qx unit to extend the  $\pi$  conjugated plane of the molecule, and developed a wide bandgap D–A copolymer

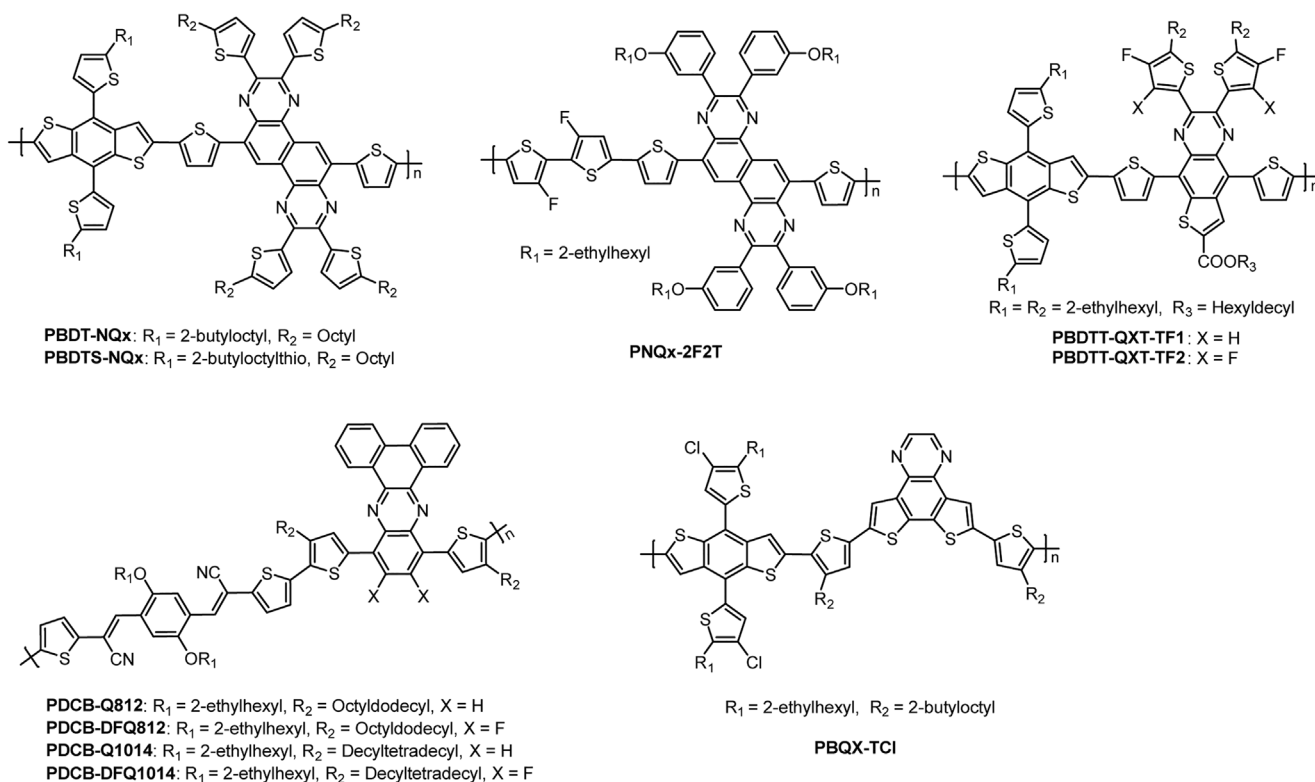


**Figure 5.** Molecular structures of the D–A copolymers based on Qx derivative as A-unit.

donor PBQx-Cl (Figure 5) with DTQx as A-unit, 2D conjugated BDT as D-unit, and an alkyl-substituted thiophene as  $\pi$ -bridges.<sup>[36]</sup> The polymer PBQx-Cl exhibits strong light absorption with a high extinction coefficient of  $9.54 \times 10^4 \text{ M}^{-1} \text{ cm}^{-1}$  in the toluene solution, and it shows a wide optical bandgap of 2.05 eV (Table 5) with absorption edge located at 605 nm. In addition, benefited from the strong electronegativity of the Cl atoms on the 2D conjugated BDT unit, the polymer PBQx-Cl shows deeper HOMO energy level of  $-5.39 \text{ eV}$ . When using

n-OS BTA3 and BTP-eC9 as acceptor, the PBQx-Cl-based binary PSCs demonstrate PCEs of 12.2% and 16.0%, respectively (Table 5). Encouragingly, the PBQx-Cl:BTA3:BTP-eC9-based ternary PSC exhibits an impressive PCE of 18.0%, which is one of the highest PCEs of the PSCs currently. In addition, the PBQx-Cl:BTA3-based PSC shows an outstanding PCE of 28.5% for a  $1 \text{ cm}^2$  device and 26.0% for a  $10 \text{ cm}^2$  device under 1000 lux LED illumination, which indicates its great potential in indoor light applications.<sup>[36]</sup>

**Table 5.** Optical properties, electronic energy levels, and photovoltaic performance parameters of the D–A copolymer donors based on Qx derivative as A-unit.

Copolymer donor	$E_{\text{opt g}}$ [eV]	HOMO [eV]	LUMO [eV]	$V_{\text{oc}}$ [V]	$J_{\text{sc}}$ [ $\text{mA cm}^{-2}$ ]	FF [%]	PCE [%]	Acceptor	Refs.
PBDT-NQx	1.80	−5.24	−3.42	0.87	16.21	64.6	9.11	ITIC	[85]
PBDTS-NQx	1.81	−5.31	−3.46	0.92	17.86	69.8	11.47	ITIC	[85]
PNQx-2F2T	1.66	−5.30	−3.37	0.80	14.3	66.0	7.5	IT-M	[86]
PDCB-Q812	1.52	−5.48	−3.15	0.89	10.90	53.30	5.19	ITIC	[87]
PDCB-DFQ812	1.62	−5.55	−3.19	1.03	13.44	58.90	8.17	ITIC	[87]
PDCB-Q1014	1.53	−5.50	−3.17	0.89	7.98	45.85	3.26	ITIC	[87]
PDCB-DFQ1014	1.56	−5.58	−3.21	1.04	10.89	62.30	7.08	ITIC	[87]
PBDTT-QXT-TF1	1.67	−5.32	−3.65	0.951	11.56	60.65	6.67	IDIC	[88]
PBDTT-QXT-TF2	1.66	−5.36	−3.70	0.975	9.78	53.61	5.12	IDIC	[88]
PBQx-TCI	2.05	−5.39	−2.86	1.24	13.3	74.2	12.2	BTA3	[36]
PBQx-TCI	2.05	−5.39	−2.86	0.82	26.0	75.2	16.0	BTP-eC9	[36]
PBQx-TCI	2.05	−5.39	−2.86	0.84	26.9	79.6	18.0	BTA3:BTP-eC9	[36]

#### 4. The Qx-Based D–A Copolymers as Hole Transport Material for Perovskite Solar Cells

Perovskite solar cells (PSCs) is also the third-generation photovoltaic technology with the advantages of low exciton binding energy, long exciton diffusion lengths, low charge carrier recombination loss in the bulk perovskite photoactive layer, and low-cost fabrication by solution processing. Therefore, it has attracted great attentions and has been developed rapidly with PCE reaching to over 25% recently, showing great potential for commercial application.<sup>[89,90]</sup> In the perovskite solar cells, the interfacial charge transport layer materials between the electrode and the perovskite photoactive layer are crucial for achieving high PCE and high stability of the devices. So far, the most widely used HTM in the n–i–p structured perovskite solar cells is spiro-OMeTAD with metal salts as dopant, however, there exists stability issue in the perovskite solar cells with the spiro-OMeTAD as HTM. In addition, due to the weak binding in the organic-inorganic hybrid perovskite and the natural instability of the organic salt compounds, the organic cations tend to escape from the perovskite crystal during thermal annealing, resulting in a nonstoichiometric balanced perovskite, which causes large amounts of defects on the grain boundaries and the surface of perovskite in the perovskite solar cells.<sup>[91]</sup> These defects are charge recombination centers, which are detrimental to the photovoltaic performance and stability of the devices. Therefore, employing high-quality HTM is critical to reduce the defects and suppress the charge recombination at the electrode interface of the perovskite solar cells.<sup>[92–94]</sup> To address these issues, the Qx-based D–A copolymers are used as HTM for highly efficient and stable perovskite solar cells recently.<sup>[92,94]</sup>

In 2018, Meng et al. employed the above-mentioned low-cost and stable D–A copolymer PTQ10 as interfacial layer for the planar n–i–p structured perovskite solar cells (Figure 6).<sup>[92]</sup> First, the polymer PTQ10 offers a deep HOMO energy level to form a good energy level alignment with the valence band of the perovskite, which facilitates the hole extraction. Second, PTQ10 serves as a hole selective layer to effectively improve the extraction and transport of the holes. Most importantly, the polymer PTQ10 acts as a dense polymeric anchor layer to suppress the volatilization of organic cations during the thermal annealing process. This cation-preserving phase conversion function prevents the escape of surface cations and ensures the stoichiometric balance of perovskite crystal. In consequence, an impressive PCE of 21.2% (Figure 6) is achieved in the planar n–i–p structured perovskite solar cells. In addition, the device exhibits significantly improved thermal stability due to the improved

perovskite film quality and the exclusion of metal salts in the hole transport layer.

However, due to the limited conductivity of PTQ10, the dual hole transport layers with a combination of PTQ10 and the traditional doped PTAA have to be utilized to simultaneously fulfill the full coverage of the perovskite surface and the efficient cascade energy transfer, which increases the complexity of device processing.<sup>[92]</sup> Very recently, Lu et al. employed three above-mentioned highly efficient Qx-based D–A copolymers PBQ5, PBQ6, and PBQ10 (see Figure 2) as the single dopant-free HTM in the planar n–i–p structured perovskite solar cells in considering their appropriate electronic energy levels and high hole mobilities.<sup>[94]</sup> The three copolymers show low-lying HOMO energy levels, and PBQ6 has the lowest HOMO energy level and the best alignment with perovskite photoactive layer based on (FAPbI<sub>3</sub>)<sub>0.98</sub>(MAPbBr<sub>3</sub>)<sub>0.02</sub>. Importantly, PBQ6 possesses relatively better film thickness tolerance up to 90 nm due to its higher hole mobility. The perovskite solar cells based on the dopant-free polymer PBQ6 as HTM demonstrates a high PCE of 22.6% with high V<sub>oc</sub> of 1.13 V and high FF of 80.8%, which is the highest PCE of the perovskite solar cells based on the dopant-free D–A copolymer HTM at the time of publication. In addition, due to the good film forming property and film thickness tolerance, PBQ6 exhibits outstanding processability with blade coating technique, and the large-area devices of 1 cm<sup>2</sup> with blade-coated PBQ6 hole transport layer also achieved high PCE of 21.1%.<sup>[94]</sup> Moreover, due to the intrinsically better stability and dopant-free characteristic of the polymer HTM, the devices with polymer PBQ6 as HTM show significantly enhanced ambient, thermal, and light-soaking stability,<sup>[94]</sup> making PBQ6 a promising HTM for potential commercialization of the perovskite solar cells.

#### 5. Summary and Outlook

We have comprehensively summarized and discussed the Qx-based D–A copolymers for the applications as polymer donor in the PSCs and as HTM in the perovskite solar cells in this review. First, the common physicochemical properties and synthetic method of the Qx unit are presented. Then, molecular design strategies of the Qx-based D–A copolymer donors for PSCs with non-fullerene *n*-OS small molecule as acceptors are discussed systematically from the aspects of backbone modulation, side chain optimization, and functional substitution with representative copolymer examples, to understand their molecular structures–photovoltaic properties relationship. Subsequently, a class of

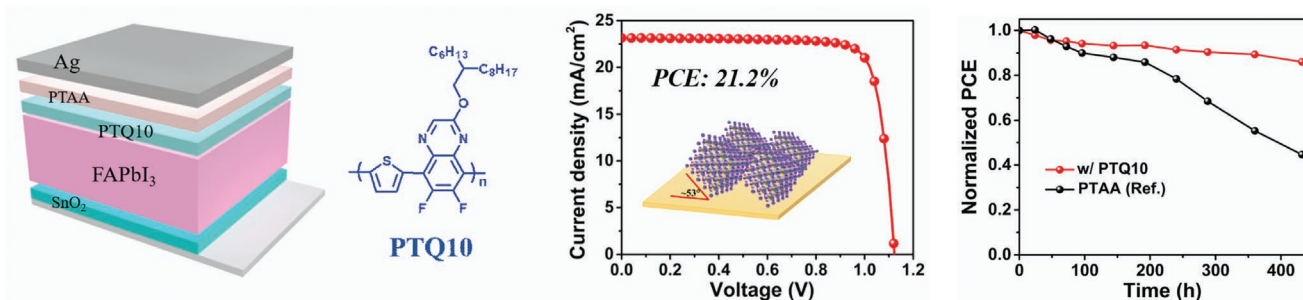


**Figure 6.** Device structure, photovoltaic performance, and stability of the perovskite solar cells employing the Qx-based D–A copolymer PTQ10 as HTM. Reproduced with permission.<sup>[92]</sup> Copyright 2018, American Chemical Society.

low-cost and high-performance D–A copolymer donor (PTQ derivatives) based on thiophene D-unit and Qx A-unit, as well as the D–A copolymer donors with Qx derivative as A-unit, are depicted, respectively. Finally, the research progress for the application of the Qx-based D–A copolymer as HTM in the pero-SCs are introduced and analyzed.

Benefiting from the unique advantages of the Qx unit that possesses suitable electronic properties and multiple substitution sites for functional optimization, researchers have put great efforts into the exploitation of high-performance Qx-based D–A copolymer donors and significantly improved the photovoltaic performance of the corresponding PSCs. At present, PCE of the single junction PSCs using the Qx-based D–A copolymers as electron donor has reached close to 18%, indicating their remarkable potential for pursuing high efficiency of the PSCs. Among the numerous excellent Qx-based D–A copolymer donors, the PTQ derivatives are the kind of most promising polymer donors for commercial application of the PSCs because of their dual advantages of low-cost and high photovoltaic performance. On the other hand, by employing the Qx-based D–A copolymers as HTM, the photovoltaic performance and stability of the pero-SCs can be significantly improved.

The commercial application of the PSCs requires the realization of high efficiency, low cost, and high stability simultaneously. Despite the great achievements, there are still huge challenges for the commercial application of the PSCs based on the Qx-based D–A copolymers. At present, a crucial limitation that causes the relatively lower PCE of the PSCs than that of the silicon-based solar cells and the pero-SCs is its relatively higher  $V_{\text{loss}}$ . Therefore, a deeper understanding of the correlation between the  $V_{\text{loss}}$  and the molecular structures of the Qx-based D–A copolymer donors is crucial for further improving the PCEs of the PSCs. For instance, we need to study what are the key properties of the molecules that can help to achieve low nonradiative recombination loss and thus realize low  $V_{\text{loss}}$ . In addition, although lower  $V_{\text{loss}}$  values have been reported recently, the corresponding PSCs usually show lower  $J_{\text{sc}}$  or FF due to the poor exciton dissociation and charge transport. Thus, it is critical to develop the excellent photovoltaic materials that can simultaneously realize high  $V_{\text{oc}}$  with low  $V_{\text{loss}}$ , large  $J_{\text{sc}}$ , and high FF, affording high PCEs. Moreover, microscopic morphology of the photoactive layer plays a critical role in determining the photovoltaic performance of the PSCs, which is affected by various factors, such as the solubility, crystallinity, and the miscibility of the donor and acceptor, etc. Therefore, understanding the inherent properties of the Qx-based D–A copolymers is helpful to design well-matched polymer donors that tend to form tight  $\pi$ – $\pi$  molecular stacking, proper domain size, high domain purity, and appropriate vertical phase separation in corresponding blend films, for matching with the low bandgap small molecule acceptors to realize high photovoltaic performance of the PSCs. Furthermore, developing high-performance Qx-based D–A copolymer donors with high tolerance of the film thickness is essential for the large-scale manufacture of the PSCs, as the film thickness fluctuation is unavoidable in the high-speed roll-to-roll manufacture of the photoactive layers of the PSCs in future application.

In addition, cost of the photoactive molecules is one of the most important issues that must be considered for commercial

application of the PSCs. To obtain low-cost and high-performance photovoltaic materials, the most effective way is to design and synthesize the photovoltaic materials that possess simple molecular structures, short synthetic route and high synthetic yield from cheap raw materials. For the Qx-based D–A copolymer donors, the easiest and most direct method is to further modify the molecular structure and further improve the photovoltaic performance of the low-cost PTQ derivatives. Moreover, improving the synthetic method of the PTQ derivative donors is believed to be useful for further reducing the synthetic cost of the polymers.

Stability of the PSCs is the most striking weakness for the commercial application currently. It is related to the stability of the photoactive molecules, interface layer molecules, electrodes, the microscopic morphology stability of the photoactive layers, and the environmental stability of the devices. Although the Qx-based D–A copolymer donors possess good chemical stability and thermal stability, the stability of the corresponding PSCs has seldom been studied. Therefore, it is of practical significance to enhance the research on the stability of the PSCs with the Qx-based D–A copolymer as donor, such as the microscopic morphology stability of the photoactive layers, water and air stability of the device, light and thermal stability of the devices, etc.

For the pero-SCs, obtaining high-quality perovskite film in both bulk and surface is critical for suppressing charge recombination, and improving the photovoltaic performance and stability of the devices. To address these issues, it is important to develop more excellent Qx-based D–A copolymers that possess more suitable energy level alignment with the valence band of the perovskite and higher hole mobility for the applications as HTM in the pero-SCs.

We anticipate that more excellent Qx-based D–A copolymers will be developed through fine molecular structure optimization in the future, which will push forward the PSCs and pero-SCs from the laboratory to the factory.

## Acknowledgements

C.S. and C.Z. contributed equally to this work. This work was supported by the National Key Research and Development Program of China (No. 2019YFA0705900) funded by MOST, the National Natural Science Foundation of China (Nos. 51820105003, 21734008, and 61904181), the Natural Science Foundation of Henan (No. 212300410284), and the Basic and Applied Basic Research Major Program of Guangdong Province (No. 2019B030302007).

## Conflict of Interest

The authors declare no conflict of interest.

## Keywords

D–A copolymers, hole transport materials for perovskite solar cells, polymer donors, polymer solar cells, quinoxaline

Received: May 31, 2021  
Revised: August 20, 2021  
Published online:

- [1] G. Yu, J. Gao, J. C. Hummelen, F. Wudl, A. J. Heeger, *Science* **1995**, 270, 1789.
- [2] Y. Li, *Acc. Chem. Res.* **2012**, 45, 723.
- [3] G. Li, R. Zhu, Y. Yang, *Nat. Photonics* **2012**, 6, 153.
- [4] P. Cheng, G. Li, X. Zhan, Y. Yang, *Nat. Photonics* **2018**, 12, 131.
- [5] Q. Wei, W. Liu, M. Leclerc, J. Yuan, H. Chen, Y. Zou, *Sci. China: Chem.* **2020**, 63, 1352.
- [6] H. Yao, L. Ye, H. Zhang, S. Li, S. Zhang, J. Hou, *Chem. Rev.* **2016**, 116, 7397.
- [7] M. C. Scharber, D. Mühlbacher, M. Koppe, P. Denk, C. Waldauf, A. J. Heeger, C. J. Brabec, *Adv. Mater.* **2006**, 18, 789.
- [8] Y. J. Cheng, S. H. Yang, C. S. Hsu, *Chem. Rev.* **2009**, 109, 5868.
- [9] T. Xu, L. Yu, *Mater. Today* **2014**, 17, 11.
- [10] C. Cui, Y. Li, *Energy Environ. Sci.* **2019**, 12, 3225.
- [11] Y. He, Y. Li, *Phys. Chem. Chem. Phys.* **2011**, 13, 1970.
- [12] Y. Lin, J. Wang, Z.-G. Zhang, H. Bai, Y. Li, D. Zhu, X. Zhan, *Adv. Mater.* **2015**, 27, 1170.
- [13] J. Yuan, Y. Zhang, L. Zhou, G. Zhang, H.-L. Yip, T.-K. Lau, X. Lu, C. Zhu, H. Peng, P. A. Johnson, M. Leclerc, Y. Cao, J. Ulanski, Y. Li, Y. Zou, *Joule* **2019**, 3, 1140.
- [14] Y. He, H.-Y. Chen, J. Hou, Y. Li, *J. Am. Chem. Soc.* **2010**, 132, 1377.
- [15] J.-D. Chen, C. Cui, Y.-Q. Li, L. Zhou, Q.-D. Ou, C. Li, Y. Li, J.-X. Tang, *Adv. Mater.* **2015**, 27, 1035.
- [16] Q. Fan, W. Su, Y. Wang, B. Guo, Y. Jiang, X. Guo, F. Liu, T. P. Russell, M. Zhang, Y. Li, *Sci. China: Chem.* **2018**, 61, 531.
- [17] R. Ma, T. Liu, Z. Luo, Q. Guo, Y. Xiao, Y. Chen, X. Li, S. Luo, X. Lu, M. Zhang, Y. Li, H. Yan, *Sci. China: Chem.* **2020**, 63, 325.
- [18] E. E. Havinga, W. Hoeve, H. Wynberg, *Polym. Bull.* **1992**, 29, 119.
- [19] C. Duan, F. Huang, Y. Cao, *J. Mater. Chem.* **2012**, 22, 10416.
- [20] D. Gedefaw, M. Prosa, M. Bolognesi, M. Seri, M. R. Andersson, *Adv. Energy Mater.* **2017**, 7, 1700575.
- [21] C. Sun, S. Qin, R. Wang, S. Chen, F. Pan, B. Qiu, Z. Shang, L. Meng, C. Zhang, M. Xiao, C. Yang, Y. Li, *J. Am. Chem. Soc.* **2020**, 142, 1465.
- [22] D. Gedefaw, M. Tassarolo, M. Prosa, M. Bolognesi, P. Henriksson, W. Zhuang, M. Seri, M. Muccini, M. R. Andersson, *Sol. Energy Mater. Sol. Cells* **2016**, 144, 150.
- [23] M. Seri, D. Gedefaw, M. Prosa, M. Tassarolo, M. Bolognesi, M. Muccini, M. R. Andersson, *J. Polym. Sci., Part A: Polym. Chem.* **2017**, 55, 234.
- [24] A. Gadisa, W. Mammo, L. M. Andersson, S. Admassie, F. Zhang, M. R. Andersson, O. Inganäs, *Adv. Funct. Mater.* **2007**, 17, 3836.
- [25] E. Wang, L. Hou, Z. Wang, S. Hellstrom, F. Zhang, O. Inganäs, M. R. Andersson, *Adv. Mater.* **2010**, 22, 5240.
- [26] Y. Kim, H. R. Yeom, J. Y. Kim, C. Yang, *Energy Environ. Sci.* **2013**, 6, 1909.
- [27] D. Dang, W. Chen, S. Himmelberger, Q. Tao, A. Lundin, R. Yang, W. Zhu, A. Salleo, C. Müller, E. Wang, *Adv. Energy Mater.* **2014**, 4, 1400680.
- [28] Q. Fan, Y. Liu, M. Xiao, H. Tan, Y. Wang, W. Su, D. Yu, R. Yang, W. Zhu, *Org. Electron.* **2014**, 15, 3375.
- [29] Q. Fan, Y. Liu, H. Jiang, W. Su, L. Duan, H. Tan, Y. Li, J. Deng, R. Yang, W. Zhu, *Org. Electron.* **2016**, 33, 128.
- [30] J. Yuan, L. Qiu, Z. Zhang, Y. Li, Y. He, L. Jiang, Y. Zou, *Chem. Commun.* **2016**, 52, 6881.
- [31] Q. Fan, H. Jiang, Y. Liu, W. Su, H. Tan, Y. Wang, R. Yang, W. Zhu, *J. Mater. Chem. C* **2016**, 4, 2606.
- [32] Y. Li, S. J. Ko, Y. P. Song, H. Choi, T. L. Nguyen, M. A. Uddin, T. Kim, S. Hwang, Y. K. Jin, Y. W. Han, *J. Mater. Chem. A* **2016**, 4, 9967.
- [33] S. Xu, L. Feng, J. Yuan, V. Cimrova, G. Chen, Z.-G. Zhang, Y. Li, H. Peng, Y. Zou, *Org. Electron.* **2017**, 50, 7.
- [34] D. Liu, W. Zhao, S. Zhang, L. Ye, Z. Zheng, Y. Cui, Y. Chen, J. Hou, *Macromolecules* **2015**, 48, 5172.
- [35] Z. Zhao, Y. Zhang, Y. Wang, X. Qin, J. Wu, J. Hou, *Org. Electron.* **2016**, 28, 178.
- [36] Y. Xu, Y. Cui, H. Yao, T. Zhang, J. Zhang, L. Ma, J. Wang, Z. Wei, J. Hou, *Adv. Mater.* **2021**, 23, 2101090.
- [37] G. Chai, Y. Chang, J. Zhang, X. Xu, L. Yu, X. Zou, X. Li, Y. Chen, S. Luo, B. Liu, F. Bai, Z. Luo, H. Yu, J. Liang, T. Liu, K. S. Wong, H. Zhou, Q. Peng, H. Yan, *Energy Environ. Sci.* **2021**, 14, 3469.
- [38] C. Sun, F. Pan, H. Bin, J. Zhang, L. Xue, B. Qiu, Z. Wei, Z.-G. Zhang, Y. Li, *Nat. Commun.* **2018**, 9, 743.
- [39] Y. Wu, Y. Zheng, H. Yang, C. Sun, Y. Dong, C. Cui, H. Yan, Y. Li, *Sci. China: Chem.* **2020**, 63, 265.
- [40] C. Sun, F. Pan, S. Chen, R. Wang, R. Sun, Z. Shang, B. Qiu, J. Min, M. Lv, L. Meng, C. Zhang, M. Xiao, C. Yang, Y. Li, *Adv. Mater.* **2019**, 31, 1905480.
- [41] D. Yuan, F. Pan, L. Zhang, H. Jiang, M. Chen, W. Tang, G. Qin, Y. Cao, J. Chen, *Sol. RRL* **2020**, 4, 2000062.
- [42] W.-H. Tseng, H.-C. Chen, Y.-C. Chien, C.-C. Liu, Y.-K. Peng, Y.-S. Wu, J.-H. Chang, S.-H. Liu, S.-W. Chou, C.-L. Liu, Y.-H. Chen, C.-I. Wu, P.-T. Chou, *J. Mater. Chem. A* **2014**, 2, 20203.
- [43] C.-H. Chen, C.-H. Hsieh, M. Dubosc, Y.-J. Cheng, C.-S. Hsu, *Macromolecules* **2010**, 43, 697.
- [44] O. Hinsberg, *Ber. Dtsch. Chem. Ges.* **1884**, 17, 318.
- [45] Z. Shang, L. Zhou, C. Sun, L. Meng, W. Lai, J. Zhang, W. Huang, Y. Li, *Sci. China: Chem.* **2021**, 64, 1031.
- [46] D. Kitazawa, N. Watanabe, S. Yamamoto, J. Tsukamoto, *Appl. Phys. Lett.* **2009**, 95, 053701.
- [47] N. Gasparini, A. Katsouras, M. I. Prodromidis, A. Avgeropoulos, D. Baran, M. Salvador, S. Fladischer, E. Spiecker, C. L. Chochos, T. Ameri, C. J. Brabec, *Adv. Funct. Mater.* **2015**, 25, 4898.
- [48] W. Huang, M. Li, L. Zhang, T. Yang, Z. Zhang, H. Zeng, X. Zhang, L. Dang, Y. Liang, *Chem. Mater.* **2016**, 28, 5887.
- [49] D. Gedefaw, M. Tassarolo, W. Zhuang, R. Kroon, E. Wang, M. Bolognesi, M. Seri, M. Muccini, M. R. Andersson, *Polym. Chem.* **2014**, 5, 2083.
- [50] D. Dang, M. Xiao, P. Zhou, J. Shi, Q. Tao, H. Tan, Y. Wang, X. Bao, Y. Liu, E. Wang, R. Yang, W. Zhu, *Org. Electron.* **2014**, 15, 2876.
- [51] J. Yuan, L. Qiu, Z.-G. Zhang, Y. Li, Y. Chen, Y. Zou, *Nano Energy* **2016**, 30, 312.
- [52] J. Yang, M. A. Uddin, Y. Tang, Y. Wang, Y. Wang, H. Su, R. Gao, Z.-K. Chen, J. Dai, H. Y. Woo, X. Guo, *ACS Appl. Mater. Interfaces* **2018**, 10, 23235.
- [53] M. Yasa, S. Goker, L. Toppare, *Polym. Bull.* **2020**, 77, 2443.
- [54] B. A. Alqurashy, B. M. Altayeb, S. Y. Alfaifi, M. Alawad, A. Iraqi, I. Ali, *Coatings* **2020**, 10, 1098.
- [55] R. P. Wardani, M. Jeong, S. W. Lee, D. R. Whang, J. H. Kim, D. W. Chang, *Dyes Pigm.* **2021**, 192, 109346.
- [56] J. Zhou, B. Zhang, W. Zou, A. Tang, Y. Geng, Q. Zeng, Q. Guo, E. Zhou, *Sustainable Energy Fuels* **2020**, 4, 5665.
- [57] L. Wang, H. Liu, Z. Huai, Y. Li, S. Yang, *Dyes Pigm.* **2018**, 148, 72.
- [58] V. Tamilavan, S. Jang, J. Lee, R. Agneeswari, J. H. Kwon, J. H. Kim, Y. Jin, S. H. Park, *Polymer* **2020**, 194, 122408.
- [59] D. Gedefaw, M. Tassarolo, M. Prosa, M. Bolognesi, P. Henriksson, W. Zhuang, M. Seri, M. Muccini, M. R. Andersson, *Sol. Energy Mater. Sol. Cells* **2016**, 144, 150.
- [60] M. Bolognesi, D. Gedefaw, D. Dang, P. Henriksson, W. Zhuang, M. Tassarolo, E. Wang, M. Muccini, M. Seri, M. R. Andersson, *RSC Adv.* **2013**, 3, 24543.
- [61] J.-H. Kim, C. E. Song, H. U. Kim, A. C. Grimsdale, S.-J. Moon, W. S. Shin, S. K. Choi, D.-H. Hwang, *Chem. Mater.* **2013**, 25, 2722.
- [62] L. Wang, H. Liu, Z. Huai, S. Yang, *ACS Appl. Mater. Interfaces* **2017**, 9, 28828.
- [63] L. Li, L. Feng, J. Yuan, H. Peng, Y. Zou, Y. Li, *Chem. Phys. Lett.* **2018**, 696, 19.
- [64] V. Tamilavan, J. Lee, J. H. Kwon, S. Jang, I. Shin, R. Agneeswari, J. H. Jung, Y. Jin, S. H. Park, *Polymer* **2019**, 172, 305.
- [65] S. Xu, L. Feng, J. Yuan, Z.-G. Zhang, Y. Li, H. Peng, Y. Zou, *ACS Appl. Mater. Interfaces* **2017**, 9, 18816.

- [66] T. Wang, T.-K. Lau, X. Lu, J. Yuan, L. Feng, L. Jiang, W. Deng, H. Peng, Y. Li, Y. Zou, *Macromolecules* **2018**, *51*, 2838.
- [67] S. Xu, X. Wang, L. Feng, Z. He, H. Peng, V. Cimrova, Y. Jun, Z.-G. Zhang, Y. Li, Y. Zou, *J. Mater. Chem. A* **2018**, *6*, 3074.
- [68] J. Yuan, Y. Liu, C. Zhu, P. Shen, M. Wan, L. Feng, Y. Zou, *Acta Phys.-Chim. Sin.* **2018**, *34*, 1272.
- [69] L. Zeng, R. Ma, Q. Zhang, T. Liu, Y. Xiao, K. Zhang, S. Cui, W. Zhu, X. Lu, H. Yan, Y. Liu, *Mater. Chem. Front.* **2021**, *5*, 1906.
- [70] C. Sun, F. Pan, B. Qiu, S. Qin, S. Chen, Z. Shang, L. Meng, C. Yang, Y. Li, *Chem. Mater.* **2020**, *32*, 3254.
- [71] C. Zhu, L. Meng, J. Zhang, S. Qin, W. Lai, B. Qiu, J. Yuan, Y. Wan, W. Huang, Y. Li, *Adv. Mater.* **2021**, *33*, 2100474.
- [72] Y. Luo, Y. Luo, X. Huang, S. Liu, Z. Cao, L. Guo, Q. Li, Y.-P. Cai, Y. Wang, *Macromol. Rapid Commun.* **2020**, *42*, 2000683.
- [73] P. Yang, M. Yuan, D. F. Zeigler, S. E. Watkins, J. A. Lee, C. K. Luscombe, *J. Mater. Chem. C* **2014**, *2*, 3278.
- [74] H. Wu, B. Zhao, W. Wang, Z. Guo, W. Wei, Z. An, C. Gao, H. Chen, B. Xiao, Y. Xie, H. Wu, Y. Cao, *J. Mater. Chem. A* **2015**, *3*, 18115.
- [75] M. Wang, D. Ma, K. Shi, S. Shi, S. Chen, C. Huang, Z. Qiao, Z.-G. Zhang, Y. Li, X. Li, H. Wang, *J. Mater. Chem. A* **2015**, *3*, 2802.
- [76] Z. Zheng, O. M. Awartani, B. Gautam, D. Liu, Y. Qin, W. Li, A. Bataller, K. Gundogdu, H. Ade, J. Hou, *Adv. Mater.* **2017**, *29*, 1604241.
- [77] S. Keum, S. Song, H. W. Cho, C. B. Park, S. S. Park, W.-K. Lee, J. Y. Kim, Y. Jin, *Synth. Met.* **2021**, *272*, 116655.
- [78] R. Lenaerts, D. Devisscher, G. Pirotte, S. Gielen, S. Mertens, T. Cardeynals, B. Champagne, L. Lutsen, D. Vanderzande, P. Adriaensens, P. Verstappen, K. Vandewal, W. Maes, *Dyes Pigm.* **2021**, *181*, 108577.
- [79] S. L. Handoko, M. Jeong, D. R. Whang, J. H. Kim, D. W. Chang, *J. Mater. Chem. A* **2020**, *8*, 19513.
- [80] C. P. Sagita, J. H. Lee, S. W. Lee, D. R. Whang, J. H. Kim, D. W. Chang, *J. Power Sources* **2021**, *491*, 229588.
- [81] C. Li, J. Zhou, J. Song, J. Xu, H. Zhang, X. Zhang, J. Guo, L. Zhu, D. Wei, G. Han, J. Min, Y. Zhang, Z. Xie, Y. Yi, H. Yan, F. Gao, F. Liu, Y. Sun, *Nat. Energy* **2021**, *6*, 605.
- [82] S. Qin, Z. Jia, L. Meng, C. Zhu, W. Lai, J. Zhang, W. Huang, C. Sun, B. Qiu, Y. Li, *Adv. Funct. Mater.* **2021**, *31*, 2102361.
- [83] E. Jo, J. B. Park, W.-H. Lee, J.-H. Kim, I. H. Jung, D.-H. Hwang, I.-N. Kang, *J. Polym. Sci., Part A: Polym. Chem.* **2016**, *54*, 2804.
- [84] S. J. Jeon, S. J. Nam, Y. W. Han, T. H. Lee, D. K. Moon, *Polym. Chem.* **2017**, *8*, 2979.
- [85] T. Yu, X. Xu, G. Zhang, J. Wan, Y. Li, Q. Peng, *Adv. Funct. Mater.* **2017**, *27*, 1701491.
- [86] S. Pang, L. Liu, X. Sun, S. Dong, Z. Wang, R. Zhang, Y. Guo, W. Li, N. Zheng, C. Duan, F. Huang, Y. Cao, *Macromol. Rapid Commun.* **2019**, *40*, 1900120.
- [87] B. He, Q. Yin, X. Yang, L. Liu, X. Jiang, J. Zhang, F. Huang, Y. Cao, *J. Mater. Chem. C* **2017**, *5*, 8774.
- [88] Y. Zhang, P. Zhou, J. Wang, X. Zhan, X. Chen, *Dyes Pigm.* **2020**, *174*, 108022.
- [89] S. D. Stranks, G. E. Eperon, G. Grancini, C. Menelaou, M. J. P. Alcocer, T. Leijtens, L. M. Herz, A. Petrozza, H. J. Snaith, *Science* **2013**, *342*, 341.
- [90] J. J. Yoo, G. Seo, M. R. Chua, T. G. Park, Y. Lu, F. Rotermund, Y.-K. Kim, C. S. Moon, N. J. Jeon, J.-P. Correa-Baena, V. Bulovic, S. S. Shin, M. G. Bawendi, J. Seo, *Nature* **2021**, *590*, 587.
- [91] A. Dualeh, N. Tetreault, T. Moehl, P. Gao, M. K. Nazeeruddin, M. Gratzel, *Adv. Funct. Mater.* **2014**, *24*, 3250.
- [92] L. Meng, C. Sun, R. Wang, W. Huang, Z. Zhao, P. Sun, T. Huang, J. Xue, J.-W. Lee, C. Zhu, Y. Huang, Y. Li, Y. Yang, *J. Am. Chem. Soc.* **2018**, *140*, 17255.
- [93] R. Xue, M. Zhang, D. Luo, W. Chen, R. Zhu, Y. (Michael) Yang, Y. W. Li, Y. F. Li, *Sci. China: Chem.* **2020**, *63*, 987.
- [94] C. Lu, C. Zhu, C. Sun, W. Lai, S. Qin, J. Zhang, W. Huang, J. Du, Y. Wang, Y. Li, *Sci. China: Chem.* **2021**, <https://doi.org/10.1007/s11426-021-1084-y>.



**Chenkai Sun** is currently a lecturer at Zhengzhou University. He received his B.S. degree in 2015 from Zhengzhou University, and his Ph.D. degree in 2020 from the Institute of Chemistry, Chinese Academy of Sciences (ICCAS), under the supervision of Prof. Yongfang Li. His research interests are the design of high-efficiency organic photovoltaic molecules (especially the low-cost and high-performance D–A copolymer donors) and the exploration of structure–property relationship of the photoactive molecules.



**Yongfang Li** is a professor at the Institute of Chemistry, Chinese Academy of Sciences (ICCAS), and at Soochow University. He received his Ph.D. degree in 1986 from the Department of Chemistry of Fudan University. He became a staff at ICCAS in 1988, and was promoted to be a professor in 1993. He was invited to be a professor at Soochow University in 2012, and was elected as a member of the Chinese Academy of Sciences in 2013. His present research field is photovoltaic materials and devices for polymer solar cells.